



**Brookhaven
National Laboratory**

BNL-105580-2014-TECH

BNL/SNS Technical Note No. 003; BNL-105580-2014-IR

H- Charge Exchange Injection into the 1 GeV NSNS Accumulator

L. N. Blumberg

November 1996

Collider Accelerator Department
Brookhaven National Laboratory

U.S. Department of Energy

USDOE Office of Science (SC)

Notice: This technical note has been authored by employees of Brookhaven Science Associates, LLC under Contract No. DE-AC02-76CH00016 with the U.S. Department of Energy. The publisher by accepting the technical note for publication acknowledges that the United States Government retains a non-exclusive, paid-up, irrevocable, world-wide license to publish or reproduce the published form of this technical note, or allow others to do so, for United States Government purposes.

DISCLAIMER

This report was prepared as an account of work sponsored by an agency of the United States Government. Neither the United States Government nor any agency thereof, nor any of their employees, nor any of their contractors, subcontractors, or their employees, makes any warranty, express or implied, or assumes any legal liability or responsibility for the accuracy, completeness, or any third party's use or the results of such use of any information, apparatus, product, or process disclosed, or represents that its use would not infringe privately owned rights. Reference herein to any specific commercial product, process, or service by trade name, trademark, manufacturer, or otherwise, does not necessarily constitute or imply its endorsement, recommendation, or favoring by the United States Government or any agency thereof or its contractors or subcontractors. The views and opinions of authors expressed herein do not necessarily state or reflect those of the United States Government or any agency thereof.

**H⁻ CHARGE EXCHANGE INJECTION INTO THE
1 GeV NSNS ACCUMULATOR**

BNL/NSNS TECHNICAL NOTE

NO. 003

L. N. Blumberg and Y. Y. Lee

November 1, 1996

ALTERNATING GRADIENT SYNCHROTRON DEPARTMENT

H⁻ Charge Exchange Injection into the 1 GeV NSNS Accumulator

L.N. Blumberg and Y.Y. Lee

November 1, 1996

Abstract

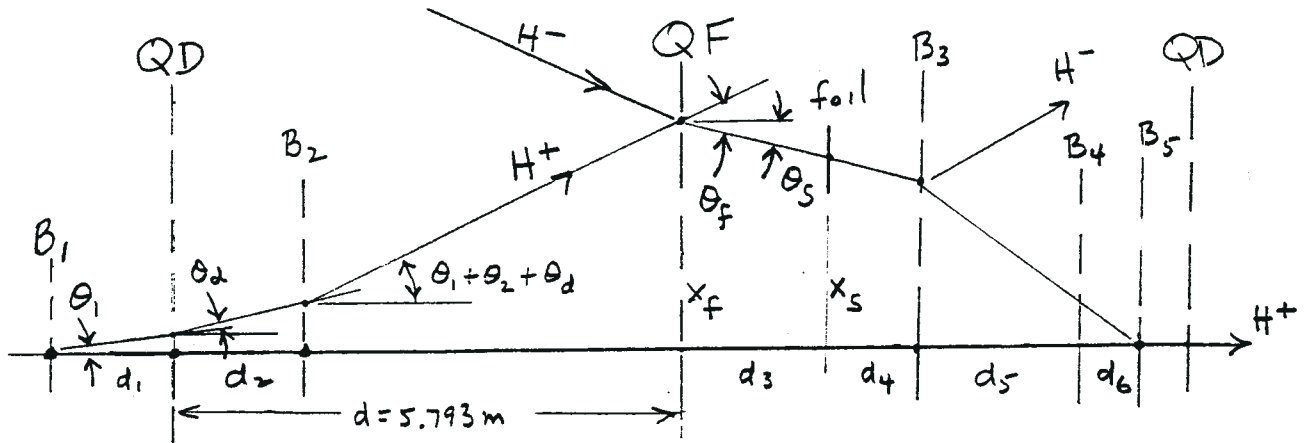
A method for efficient H⁻ injection into a tilted acceptance ellipse at the stripper foil in a FODO cell of the accumulator ring is described. A 400 $\mu\text{g}/\text{cm}^2$ C¹² foil is chosen for the stripper to obtain a high conversion fraction $f_c = f_{-1,1} = 0.9984$ for H⁻ to H⁺. Additional methods for reducing losses from nuclear scattering and reactions in the foil are discussed. Subsequent losses from magnetic field ionization of the residual H⁰ component are estimated and found to be comparable to nuclear losses. Fractional loss from H⁰ stripping is estimated to be $< 4.9 \cdot 10^{-5}$, and Monte Carlo tracking calculations give foil losses from nuclear interactions and Coulomb scattering as $4.32 \cdot 10^{-5}$. A method for sweeping and collecting the 544 keV electrons generated from ionization of the H⁻ ions in the foil is presented. Heating of the foil by energy deposition from protons and stripped electrons is estimated.

1. Layout of the Injection Straight Section.

The lattice design described by Ruggiero[1.1] provides two missing-magnet FODO cells for H⁻ injection with a horizontally focussing quadrupole QF at the center. In the present design, the trajectory of the incident H⁻ beam passes through the quadrupole aperture off-axis, as suggested by Rees[1.2], is bent parallel to the straight-section axis by the quad field, and passes through the stripper foil downstream of the quad. The equilibrium orbit of the ring is initially moved to the same off-axis position as the H⁻ beam by two upstream bump magnet B₁ and B₂ and is deflected by an equal and opposite bend in the quad to coincide with the H⁻ beam. The magnet configuration for this scheme is shown in Figure I-1. The need to locate the stripper foil in an accessible location downstream of QF, where the alpha function is non-zero, poses difficulty for this design since optimum injection

efficiency requires that the center of the ring acceptance ellipse track the ellipse axis $x' = -(\alpha/\beta)x$ as the injection bump collapses. Computer tracking calculations to compare injection losses with and without H^- beam tracking of the ellipse axis have not yet been done for the present design; however, previous studies[1.3] with a similar lattice indicate a factor of 4.5 increased loss if the ellipses center moves on the phase space trajectory $x' = 0$ rather than the ellipse axis. The orbit bump configuration proposed here accomplishes the desired phase space trajectory of the ellipse.

In the sketch below, we show the terminology used in the analysis of the local, closed orbit injection bump. Point dipoles and quadrupoles are assumed and small angle approximations are used. Quadrupole angle deflections are $\theta_{d,f} = S_{d,f} x$, where $S_{d,f} = G_{d,f} L/R$ with $G_{d,f}$ the gradient in QD or QF, L = quad effective length of 0.5 m for this lattice, and $R = B\rho$ = magnetic rigidity = 56.5737 kG-m for 1 GeV H^- . The quad gradients are $G_d = 23.7$ kG/m and $G_f = 20.9$ kG/m.



The orbit displacement and angle at quad QD are:

$$\begin{aligned} x_d &= d_1 \theta_1 \\ \theta_d &= \theta_1 d_1 S_d \end{aligned} \quad (1.1)$$

and the corresponding angles and positions after QF and at the stripper are:

$$\begin{aligned} x_f &= \theta_1(d + d_1 + d d_1 S_d) + \theta_2(d - d_2) \\ \theta_s &= \theta_1 + \theta_2 + \theta_d - x_f S_f \\ x_s &= x_f + d_3 \theta_s \end{aligned} \quad (1.2)$$

The slope S of the phase space trajectory of the orbit at the stripper is given by $\Delta\theta_s / \Delta x_s$, which is a function only of the ratio $r = \Delta\theta_2 / \Delta\theta_1$

$$S = \frac{1 + d_1(S_d - S_f) - dS_f(1 + d_1 S_d) + r[1 - S_f(d - d_2)]}{d + d_1(1 + d S_d) + d_3[1 + d_1(S_d - S_f) - dS_f(1 + d_1 S_d)] + r[d - d_2 + d_3 - d_3 S_f(d - d_2)]} \quad (1.3)$$

The betatron functions at the stripper are [1.1] $\alpha = 2.124$ and $\beta = 22.570$ m and the desired slope is then $S = -(\alpha/\beta) = -0.0941$ rad/m. We choose dimensions $d_1 = d_2 = 1.4$ m and $d_3 = 0.45$ m and obtain for the desired ratio of bump angle changes

$$r = \Delta\theta_2 / \Delta\theta_1 = -0.775 \quad (1.4)$$

The changes in θ_1 and θ_2 are thus of opposite sign to attain a negative slope. To obtain initial values for the angles θ_1 and θ_2 we choose $x_f = 0.1$ m and, for convenience, $\theta_s = 0$. Iteration of Equations 1.2 gives $\theta_1 = 5.87$ mrad and $\theta_2 = 10.88$ mrad. For final values of the bump angles, we first compute the RMS width of the beam ellipse $\sigma_B = \sqrt{\epsilon_B \beta}$ using a beam emittance $E_B = \pi \epsilon_B$ which is 1/8 of the ring acceptance $A = 470 \pi$ mm-mrad for an assumed 1 MW source [1.1]. Then $\sigma_B = 3.642$ cm which is taken as the change in orbit position x_s at the stripper. Iteration of Equations 1.2 with the constraint condition Equation 1.4 gives final angles $\theta_1 = -1.05$ mrad and $\theta_2 = 16.243$ mrad at the end of injection, and a final angle $\theta_s = 3.43$ mrad. The initial and final beam ellipses at the stripper are illustrated

in Figure I-2. The code used for computing the above angles is given in Appendix D.

Downstream of the stripper the ring orbit passes through a fixed dipole B_3 with a field of $B = 2.364$ kG chosen arbitrarily for convenience in calculating the ionization of the residual H° beam in Section 6. The choice of length of B_3 is also arbitrary; we set $L_3 = 0.8$ m and obtain a deflection of $\theta_3 = 33.43$ mrad. The initial deformed orbit trajectory then crosses the unperturbed orbit $x = 0$ at a distance $d_5 + d_6 = 2.9914$ m downstream of the center of B_3 . We locate the center of pulsed dipole B_5 at this position. An additional pulsed dipole B_4 is required upstream of B_5 to bend the collapsing orbit to an $x = 0$ value at B_5 . We choose $d_5 = 2.0$ m and $d_6 = 0.9914$ m. The final bends of B_4 and B_5 are then $\theta_4 = 24$ mrad and $\theta_5 = 6$ mrad.

References

- 1.1 A.G. Ruggiero, L. Blumberg, Y.Y. Lee, and A. Luccio, The NSNS Accumulator Ring, BNL/NSNS Technical Note TN-1 (1996).
- 1.2 Y. Cho, private communication to W.T. Weng (1995).
- 1.3 L.N. Blumberg, H^- Injection Simulation for a 5 MW Spallation Neutron Source, BNL Report BNL-60071 (1994), p. 6.

F_g. H-1

INJECTION ORBIT BUMP

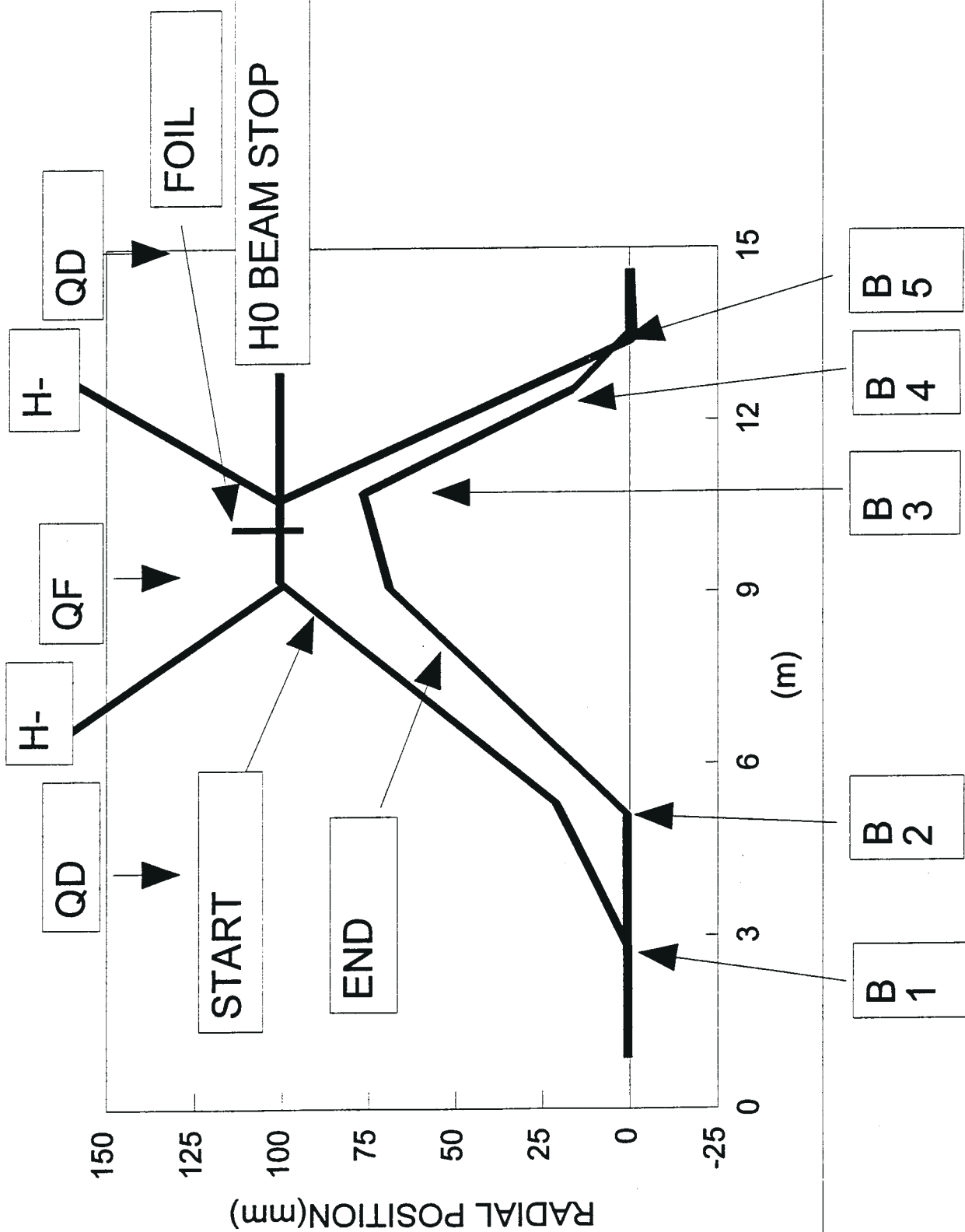
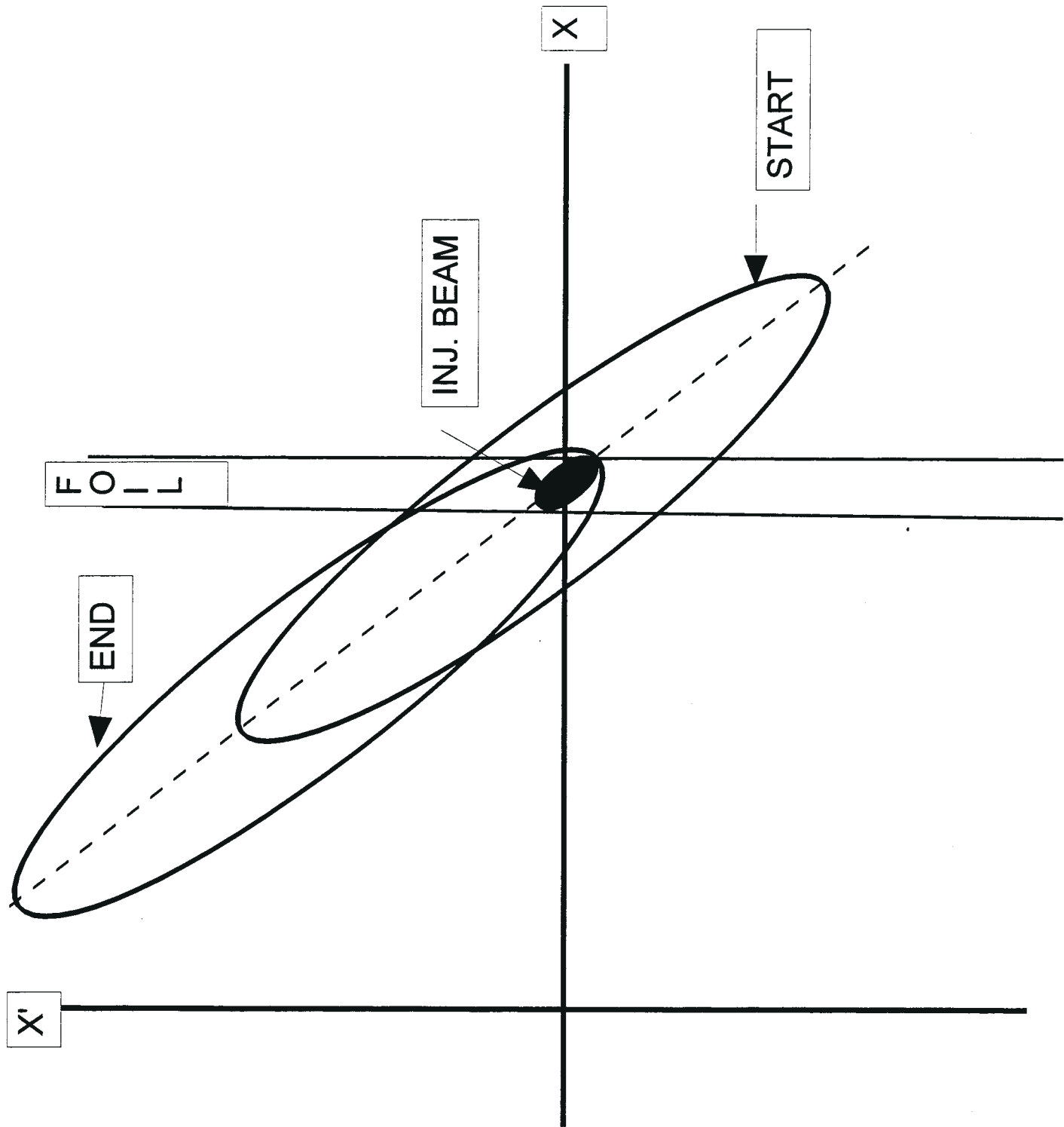


Fig. I-2



2. Magnetic Stripping of H⁻ Ions.

The stripping reaction H⁻ → H[°] + e⁻ in external magnetic fields has long been recognized as a loss mechanism in H⁻ accelerator beams. Stinson, et al.[2.1], concerned with beam loss in the planned TRIUMF H⁻ cyclotron, obtained experimental values for the constants A₁ and A₂ in the theoretical expression for the proper lifetime τ_o of the ion in an external electric field E

$$\tau_o = (A_1/E) \exp(A_2/E) \quad (2.1)$$

where the electric field in the H⁻ rest frame is related to the transverse lab magnetic field \vec{B}_\perp by the Lorentz transformation[2.2] of the field (MKS)

$$\vec{E}_\perp = \gamma \vec{v} \times \vec{B}_\perp \quad i.e., \quad E = \beta \gamma c B \quad (2.2)$$

Subsequently, Sherk[2.3] has provided a derivation of Equation 2.1 using tunneling through a potential barrier created by the electric field. Jason, Hudgings and van Dyck[2.4] have measured very precise values for the constants A₁ and A₂ which we use here

$$\begin{aligned} A_1 &= 2.47 10^{-6} \text{ V-sec/m } (\pm 4\%) \\ A_2 &= 4.49 10^9 \text{ V/m } (\pm 0.25\%) \end{aligned} \quad (2.3)$$

The lifetime τ of the ion in the lab system is given by the Lorentz transformation as $\tau = \gamma \tau_o$ and the lab stripping length λ_s, the distance traveled by the ion in time τ is

$$\lambda_s = v \tau = \beta \gamma c \tau_o \quad (2.4)$$

The fractional attenuation of a beam traversing a distance s in the field is

$$N(s)/N(o) = \exp(-s/\lambda_s) \quad (2.5)$$

and the fractional loss after traversing $s = 1$ meter is

$$f_L(1) = 1 - \exp(-1/\lambda_s) \approx 1/\lambda_s \quad (2.6)$$

We have evaluated Equation 2.6 as a function of the kinetic energy E_k of the H^- ion using Newton's iteration. E_k is related to the relativistic factor $\beta\gamma$ by

$$\beta\gamma = \sqrt{\gamma^2 - 1} = \sqrt{(E_k/M)^2 + 2(E_k/M)} \quad (2.7)$$

In Equation 2.7 $M = mc^2$ is the rest energy of the ion. The results are shown in Figure II-1 for several values of the loss fraction f_L . In particular, at $E_k = 1$ GeV, the magnetic fields giving loss fractions $f_L = 10^{-5}, 10^{-4}$ and 10^{-3} are $B = 3.545, 3.914$ and 4.366 kG, respectively. The losses are thus a rapidly increasing function of field and we have taken care in the present design of the Linac-to-ring transport and in the injection straight section not to exceed the $f_L = 10^{-5}$ field. Similar constraints are employed for the beam transport at LAMPF[2.5]. The maximum field encountered by the H^- beam in the straight section design is 2.09 kG at the QF quadrupole where the gradient is $G_f = 0.209$ kG/cm and the initial displacement of the H^- beam center is $x_f = 10$ cm.

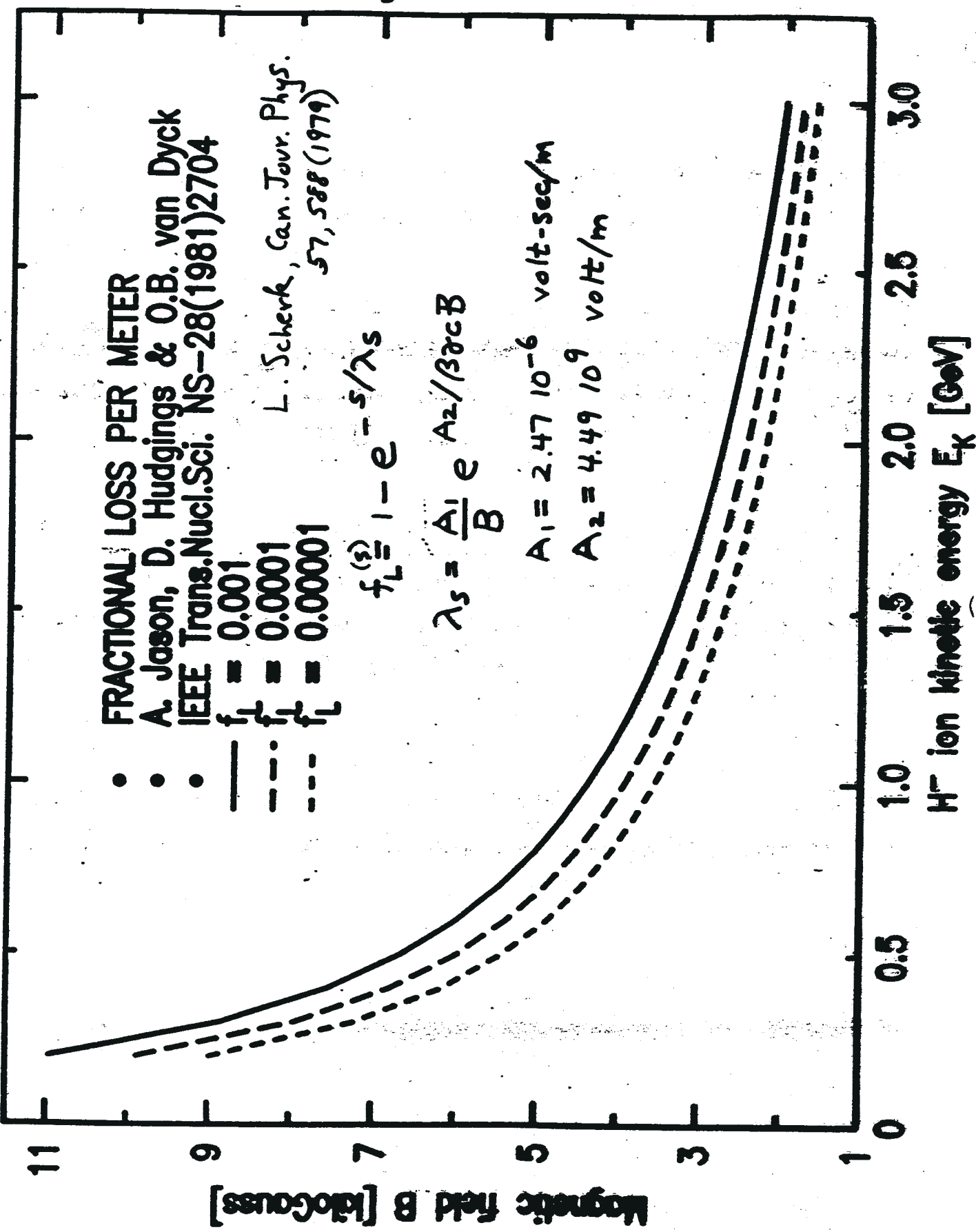
References

- 2.1 G.M. Stinson, W.C. Olsen, W.J. McDonald, P. Ford, D. Axen and E.W. Blackmore, Electric Dissociation of H⁻ Ions by Magnetic Fields. Nucl. Instrum. Meth. 74 (1969), 333.
- 2.2 See for example, W. Panofsky and M. Phillips, Classical Electricity and Magnetism. Addison-Wesley Publishing Company (1955), p. 283, Eq. 17-42.
- 2.3 L.R. Scherk, An Improved Value for the Electron Affinity of the Negative Hydrogen Ion. Can. J. Phys. 57 (1979), 558.
- 2.4 A.J. Jason, D.W. Hudgings and O.B. van Dyck, Neutralization of H⁻ Beams by Magnetic Stripping. IEEE Trans. Nucl. Sci. NS-28, No. 3 (1981), 2704.
- 2.5 R. Macek, private communication (1993). At Los Alamos they do not operate transport dipoles above 3.75 kG at 800 MeV.

H⁻ MAGNETIC STRIPPING FRACTIONAL LOSS, FIELD vs. ENERGY

- 10 -

Fig. H-1



3. Conversion Efficiency of H⁻ to H⁺ in C¹² Stripper Foil.

Joy[3.1] has obtained an expression, confirmed by Webber and Hojvat[3.2], for the fraction $f_{-1,1}$ of H⁻ converted to H⁺ in a foil of thickness t

$$f_c = f_{-1,1} = 1 - \frac{\sigma_{-1,0} e^{-\sigma_{0,1}x} - (\sigma_{0,1} - \sigma_{-1,1}) e^{-(\sigma_{-1,0} + \sigma_{-1,1})x}}{\sigma_{-1,0} + \sigma_{-1,1} - \sigma_{0,1}} \quad (3.1)$$

where $\sigma_{-1,0}$, $\sigma_{0,1}$ and $\sigma_{-1,1}$ are the microscopic cross-sections for the stripping reactions H⁻ → H⁰ + e⁻, H⁰ → H⁺ + e⁻ and H⁻ → H⁺ + 2e⁻, respectively. In Equation 3.1 $x = N_o \tau / A$ with N_o = Avogadro's number, A = atomic weight of foil atom, and $\tau = t \rho$ is the areal density of the foil. Webber and Hojvat have measured the stripping cross-sections at 200 MeV from the Fermilab Linac and their results, together with a theoretical prediction by Gillespie[3.3] are reproduced in Figure III-1. It is seen that the 200 MeV data are below the theoretical curve, although Jason reports[3.4] that the Los Alamos data at 800 MeV agree with the theoretical result. It should also be noted that Webber and Hojvat find that $\sigma_{-1,1}$ is consistent with zero at 200 MeV. We assume for the present study that $\sigma_{-1,1} = 0$ at 1 GeV and use the theoretical curve to obtain

$$\begin{aligned} \sigma_{-1,0} &\approx 8.0 \cdot 10^{-19} \text{ cm}^2 \\ \sigma_{0,1} &\approx 3.5 \cdot 10^{-19} \text{ cm}^2 \end{aligned} \quad (3.2)$$

Equation 3.1 is plotted in Figure III-2. It is seen that the unconverted fraction $1 - f_{-1,1}$ is 5×10^{-5} for a $\tau = 600 \mu\text{g/cm}^2$ foil and thus smaller than the maximum loss criterion of $f_L \leq 10^{-4}$ which we have adopted for the NSNS ring. However, thicker foils are undesirable for two reasons: (1) larger losses from Coulomb scattering and nuclear reactions as discussed in Section 5 and (2) foil heating from energy deposition which will increase with foil thickness as discussed in Section 8. The foil heating problem can be alleviated by segmenting a thicker

foil into two or three thinner foils in tandem, thereby increasing the ratio of surface area to foil volume. But nuclear interaction losses in $600 \mu\text{g}/\text{cm}^2$ will exceed our loss criterion for attainable values of multiple foil traversals by the spiraling ring beam as discussed in Section 4.

At the other extreme, say $\tau = 200 \mu\text{g}/\text{cm}^2$ foils which are used presently in the LANSCE ring[3.5] and elsewhere, the unconverted H^- beam fraction from Figure III-2 is $1 - f_c = 0.0527$. This fraction is predominantly neutral hydrogen atoms in the ground state and excited states which are difficult to eliminate and give rise to losses downstream of the stripper as discussed in Section 6. The unconverted fraction which remains as H^- ions can be estimated from the result

$$f_{\text{H}^-} = \exp(-\tau/\bar{\tau}) \quad (3.3)$$

where $\bar{\tau}$ is the mean free path in units of areal density, i.e., $\bar{\tau} = \rho\bar{\lambda} = A/N_o\sigma_{-1,0} = 25 \mu\text{g}/\text{cm}^2$. Then $f_{\text{H}^-} = 3.35 \cdot 10^{-4}$ for $\tau = 200 \mu\text{g}/\text{cm}^2$ which is negligible compared to $1 - f_c$. For the present design we have chosen $\tau = 400 \mu\text{g}/\text{cm}^2$ as a compromise between the conflicting problems noted above. At $\tau = 400 \mu\text{g}/\text{cm}^2$ the unconverted fraction of the H^- beam is $1 - f_c = 1.58 \cdot 10^{-3}$ and the surviving fraction of H^- is $f_{\text{H}^-} = 1.13 \cdot 10^{-7}$ which is negligible.

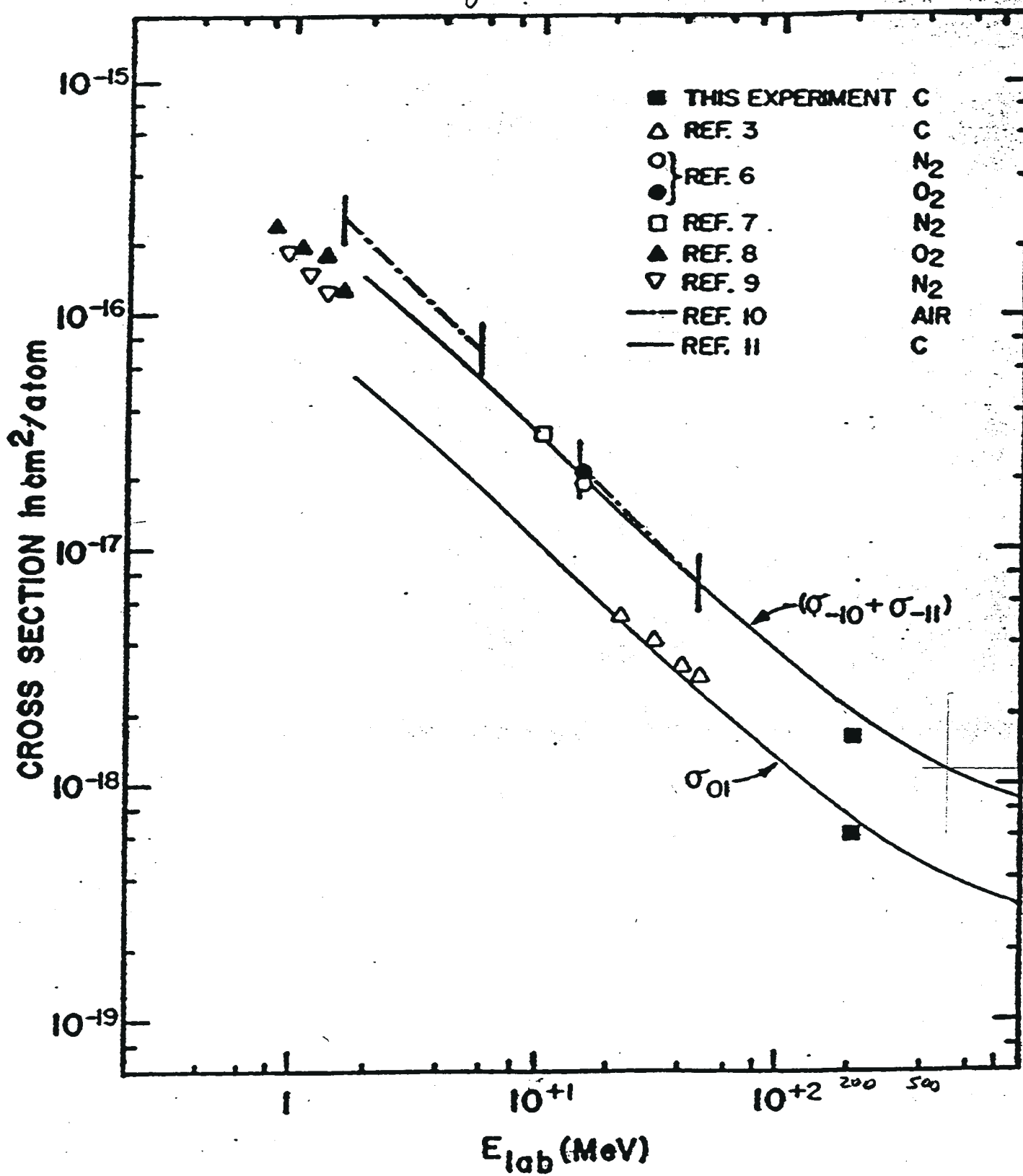
References

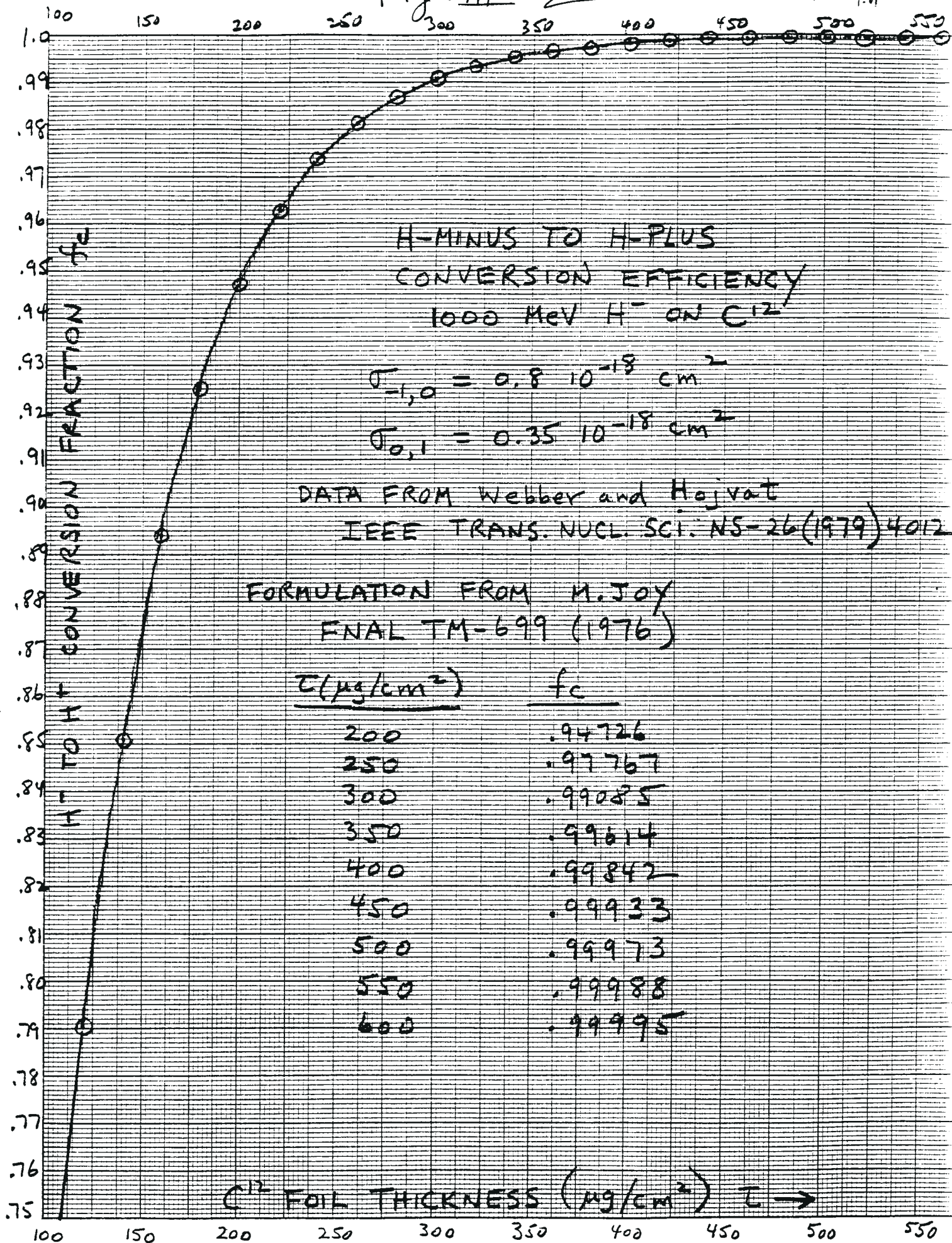
- 3.1 M. Joy, Charge Changing Methods for H^- Injection Into the Booster Synchrotron. Fermilab Technical Memo FNAL/TM-699 (1976).
- 3.2 R.C. Webber and C. Hojvat, Measurement of the Electron Loss Cross Sections for Negative Hydrogen Ions on Carbon at 200 MeV. IEEE Trans. Nucl. Sci. NS-26 (1979), 4012.

- 3.3 G.H. Gillespie, High-energy Cross Sections for H⁻ Ions Incident on Intermediate and High-Z Atoms. Phys. Rev. A16, 943 (1977) and private communication to Webber and Hojvat (1979).
- 3.4 A.J. Jason, private communication (1996).
- 3.5 M.J. Borden, G.E. Adamson, R.N. Johnson and W.F. Nicaise, Long-life Carbon-fiber-supported Stripper Foils. Nucl. Instrum. Meth. A303 (1991), 63.

WEBBER & HOJVAT IEEE Trans. Nucl. Sci. NS-26 (1979)

Fig. III-1





4. Multiple Traversals of the Stripper Foil. Smoke-ring Injection.

Following the initial traversal of the stripper by an H^- ion, the resulting proton can cross the foil on subsequent turns as it executes betatron oscillations about the collapsing closed orbit. Additional traversals result in increased probability of loss from nuclear non-elastic interactions as well as nuclear and Coulomb elastic scattering of protons out of the ring acceptance. Moreover, they contribute to additional energy deposition and thus heating and radiation damage in the foil. Traversals can be reduced using a smaller foil width, a faster initial rate of collapse of the bump, moving the collapsing orbit along the ellipse axis $x' = -(\alpha/\beta)x$, and starting injection with the ellipse center displaced from the incident H^- beam (smoke-ring). An initial estimate of the average number of traversals per injected H^- , \bar{N}_t , using the ACCSIM code[4.1] and the parameters of the present NSNS design has been made by Maletic[4.2] for a 2 cm wide C^{12} foil, linear collapsing bumps, smoke ring injection of 1200 turns, and $\tau = 400 \mu g/cm^2$. The result $\bar{N}_t = 56$ was obtained and Coulomb scattering loss out of the 470π mm-mrad acceptance was $< 10^4$. These low losses are understandable in terms of previous calculations using the HMINUSINJ code where negligible multiple Coulomb scattering loss is seen at 1.25 GeV as discussed in Section 5.

An upper limit for nuclear losses can be estimated from the $p + C^{12}$ elastic cross-section data of Palevsky, et al.[4.3] at 1 GeV. They infer from optical model fits which give the scattering amplitude, and the optical theorem which relates the total cross-section to the imaginary part of the forward amplitude, the value $\sigma_T = 370$ mb. The fraction of injected particles which undergo nuclear interactions is then

$$(f_N)_{\max} = N_o \tau \sigma_T \bar{N}_t / A = 4.16 \cdot 10^{-4} \quad (4.1)$$

This value exceeds our maximum loss criterion of 10^4 . The actual losses will be somewhat smaller since the elastic scattering distribution is strongly forward-peaked and some of the scattered protons will be within the ring acceptance as discussed in Section 5. However, we

cannot expect a major decrease from this source since the non-elastic contribution to σ_T has been measured at a number of energies up to 600 MeV by Renberg, et al.[4.4] as $\sigma_{ne} = 233$ mb at 600 MeV with little variation in this energy region. If we take that value at 1 GeV, then $\sigma_{el} = 137$ mb is only 37% of the total cross-section.

A major improvement in expected losses can be had by arranging the orbit bump to move along the ellipse axis $x' = -(\infty/\beta)x$ as discussed in Section 1. In Maletic's calculation, the orbit translated along the line $x' = 0$ and, as noted, a factor of 4.5 reduction in loss can result from the orbit bump proposed here. Another reduction in losses can be had by using a smaller foil. The foil width is determined by the fraction of incident H^- beam we wish to intercept. The present optics solution for the HEBT line gives a matched H^- spot at the stripper foil. For an expected[4.5, 4.6, 4.7] normalized RMS emittance from the Linac of $E_{N,rms} = 0.25 \pi$ mm-mrad and unnormalized value of $E_{UN,rms} = \pi\epsilon = E_{N,rms}/\beta\gamma = 0.138 \pi$ mm-mrad, and horizontal beta at the stripper of $\beta_{x,s} = 22.57$ m we have an RMS width of the H^- beam of

$$\sigma_{H^-} = \sqrt{\epsilon\beta} = 1.765 \cdot 10^{-3} m. \quad (4.2)$$

There is no contribution to the width from momentum spread since the injection straight is dispersionless[1.1]. Thus, the half-width of 1 cm for the foil used in the ACCSIM run is 5.67 σ . This is unnecessarily large since, from Figure IV-1, it is seen that essentially 100% of the H^- beam is intercepted by the foil, neglecting non-Gaussian tails. We believe that some fraction of the H^- beam missing the foil is acceptable, say 2.2%, which would result from a $\pm 2.27 \sigma$ foil width. A reduction of foil width from 2 cm to 0.8 cm should give an additional factor of 2.5 reduction in traversals and hence nuclear losses since previous calculations[4.6] indicate that losses are approximately proportional to foil size. Results of previous loss calculations are given here as Figure IV-2. It should also be noted that a smaller H^- beam spot on the foil, and thus smaller permissible foil size, could be realized since there is no compelling reason for a matched optics solution for the H^- beam at the

stripper. However, a smaller spot implies larger energy deposition per unit volume in the foil and thus greater foil heating as noted in Section 8.

Traversals can also be reduced by a more rapid initial rate of collapse of the bump. The ACCSIM calculation used a linearly decreasing bump. Previous calculations by Blumberg, et al.[1.3, 4.6] with the HMINUSINJ code used an exponential collapse, and Lee and Ratner[4.8] suggest a parabolic collapse. Another contribution to reduced losses would be inclusion of a vertical bump to move the vertical phase ellipse through the H^- beam, again along the ellipse axis $z' = -(\alpha/\beta)z$. Maletic's ACCSIM calculation did not include a vertical bump and the presently proposed scheme in Section 1 does not yet address this issue. Numerical simulations with existing codes can be done to determine whether a pulsed vertical orbit bump gives significant reduction in traversals.

Finally, we point out that particles injected near the ellipse center have a higher probability of traversing the foil on subsequent turns than particles injected at the periphery of the ellipse. Particles injected near the ellipse center have smaller betatron oscillation amplitude and remain near the ellipse center as the orbit moves across the foil. Previous calculations for 600 MeV injection into a Booster[1.3] and 1.25 GeV injection into an Accumulator[4.6] were performed by starting injection near or at the ellipse center and show the enhanced traversal effect clearly as illustrated in Figure IV-3 for 600 MeV injection. Ions injected initially experience more traversals than those later in the injection interval. The number of traversals decrease for approximately the first 25% of the injection interval. Thus, if injection had started when the ellipse center moved 25% of the distance from its center to its edge, we could eliminate those turns with large numbers of traversals/proton. This injection method leaves an unpopulated region in phase space about the ellipse center, and the scatter-plot appearance, as shown for a 1.25 GeV case in Figure IV-4, suggests the name "smoke-ring" injection. The scheme is employed in the AGS Booster and gives significant improvement in performance. Maletic's ACCSIM calculation for the present lattice used this method, although no numerical studies have been made to determine the optimum smoke-ring.

Another benefit from smoke-ring injection is the elimination of high phase space density of particles near the ellipse center which give rise to a larger space-charge tune spread than pertains for a uniform charge density. To illustrate the affect of large space-charge density at the beam center, assume a Gaussian for the radial space-charge density distribution

$$\rho(r) = en_o \exp(-\alpha r^2) \quad (4.3)$$

We can then generalize Laslett's derivation of space-charge tune shift[4.9] to obtain

$$\Delta v = [v_o - \sqrt{v_o^2 - 4F(r)}]/2 \quad (4.4)$$

where the function F(r) is given by

$$F(r) = r_p C N [1 - \exp(-\alpha r^2)] / (2\pi)^2 \beta^2 \gamma^3 B [1 - \exp(-\alpha r_m^2)] r^2 \quad (4.5)$$

In Equation 4.5, r_p = classical proton radius = $e^2/4\pi\epsilon_0 mc^2 = 1.5347 \cdot 10^{-18} m$, C = ring circumference, N = total number of protons in the ring, B = ring bunching factor and r_m = radial cut-off of the charge distribution which is related to the ring acceptance $A = \pi r_m^2/\bar{\beta}$. We can show, in the limit that the radial extent of the Gaussian $\sigma \rightarrow \infty$ where $\alpha = 1/2\sigma^2$, the tune shift from the resulting uniform space charge is the familiar Laslett expression

$$(\Delta v)_{uniform} = r_p N / 2\beta^2 \gamma^3 B A \quad (4.6)$$

and that Equation 4.6 gives the minimum tune shift for N particles in a ring of given circumference. To illustrate the radial tune dependence we plot in Figure IV-5 the tune shift

of Equation 4.4 for several choices of Gaussian width (σ_x in the figure) at 600 MeV and, in Figure IV-6, a beam profile at the same energy for a case where smoke-ring injection was not used. The central Gaussian peak in Figure IV-6 can be reduced by avoiding injection into the central region of the ellipse.

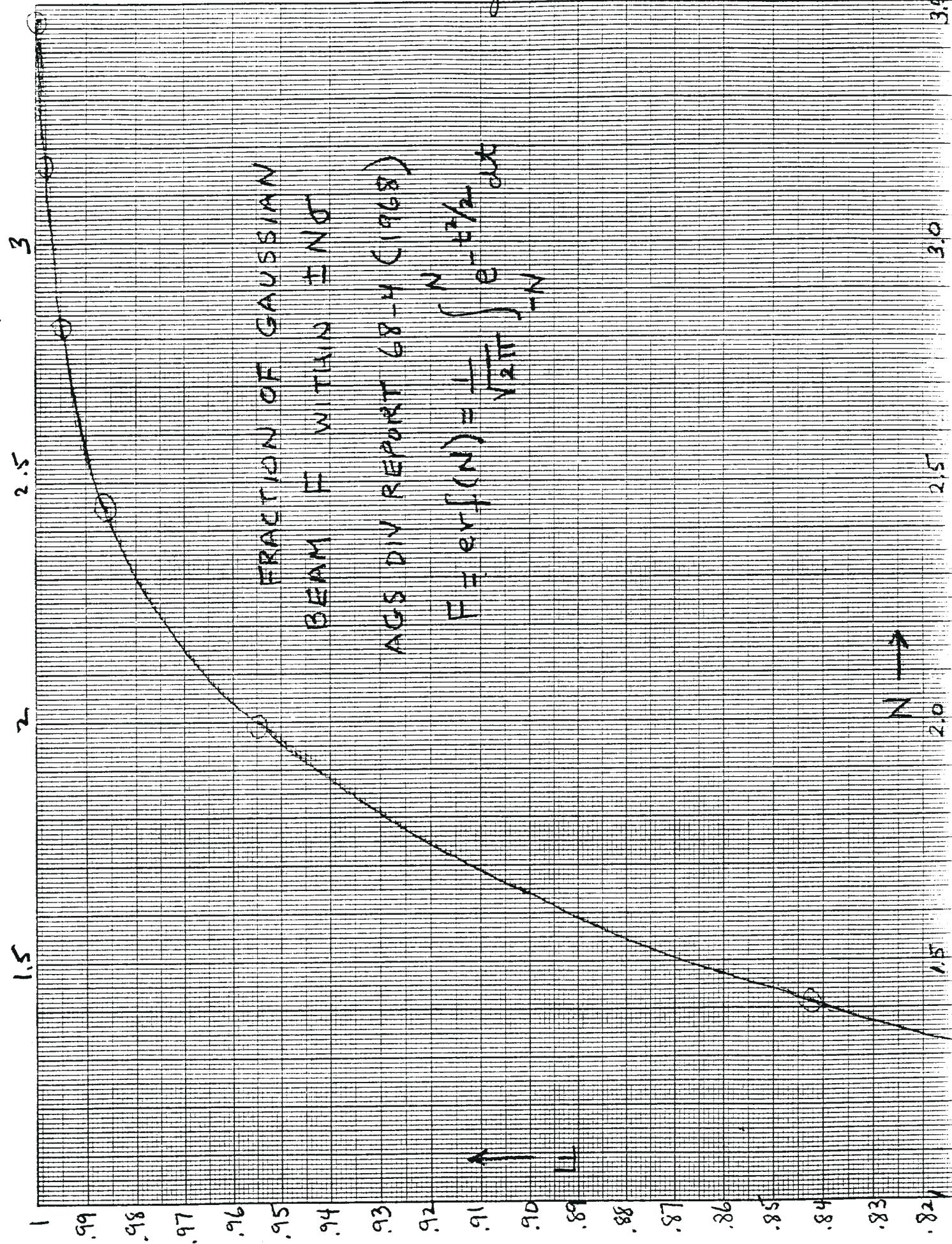
References

- 4.1 F.W. Jones, G.H. MacKenzie and H. Schonauer, ACCSIM--A Program to Simulate the Accumulation of Intense Proton Beams, Proc. 14th Int. Conference on High Energy Accelerators, Part. Accel. 31, 199 (1990). See also F.W. Jones, User's Guide to ACCSIM, TRIUMF Design Note TRI-DN-90-17 (1990).
- 4.2 D. Maletic, private communication, August 1996.
- 4.3 H. Palevsky, J.L. Friedes, R.J. Sutter, G.W. Bennett, G.J. Igo, W.D. Simpson, G.C. Phillips, D.M. Corley, N.S. Wall, R.L. Stearns and B. Gottschalk. Elastic Scattering of 1-BeV Protons from Hydrogen, Helium, Carbon and Oxygen Nuclei, Phys. Rev. Lett. 18 (1967), 1200.
- 4.4 P.U. Renberg, D.F. Measday, M. Pepin, P. Schwaller, B. Favier and C. Richard-Serre.. Reaction Cross Sections for Protons in the Energy Range 220-570 MeV, Nucl. Phys. A183 (1972), 81.
- 4.5 Private communication, T. Wangler to D. Raparia (1996). Also see report by J. Alessi in Brookhaven National Laboratory 5-MW Pulsed Spallation Neutron Source Preconceptual Design Study, A. van Steenbergen, Editor, BNL-60678 (1994), Section 4.2, p. 4.2-2.
- 4.6 L.N. Blumberg, A.U. Luccio, A. van Steenbergen and F.W. Jones. A pulsed Spallation Neutron Source Solution with a 1.25 GeV Accumulator. BNL Report BNL-62391 (1995).
- 4.7 Proc. of the Workshop on Ion Source Issues Relevant to a Pulsed Spallation Neutron Source: Part I: Workshop Summary. L. Schroeder, K-N. Leung and J. Alonso, Eds., Lawrence Berkeley Laboratory, October 24-26, 1994.

- 4.8 Y.Y. Lee and L.G. Ratner, BNL/AD Booster Technical Note 47 (June 1986). See also M. Blaskiewicz and A.U. Luccio, BNL/AD Technical Note 195A (August 1991).
- 4.9 L.J. Laslett, Proc. 1963 Summer Study on Storage Rings, Accelerators and Experiments at Super High Energy, J. Bittner, Ed., BNL Report BNL-7534 (1963). See also H. Bruck, Circular Particle Accelerators, Inst. Nat. des Sciences et Tech. Nucleaire, Saclay, France (1966). English translation: Los Alamos Report LA-TR-72-10 Rev. (1972), Chapt. XXVII.

6/5/96 Roy B

- 22 -
 Fig. Hr-1



- 23 -
Fig. IV-2

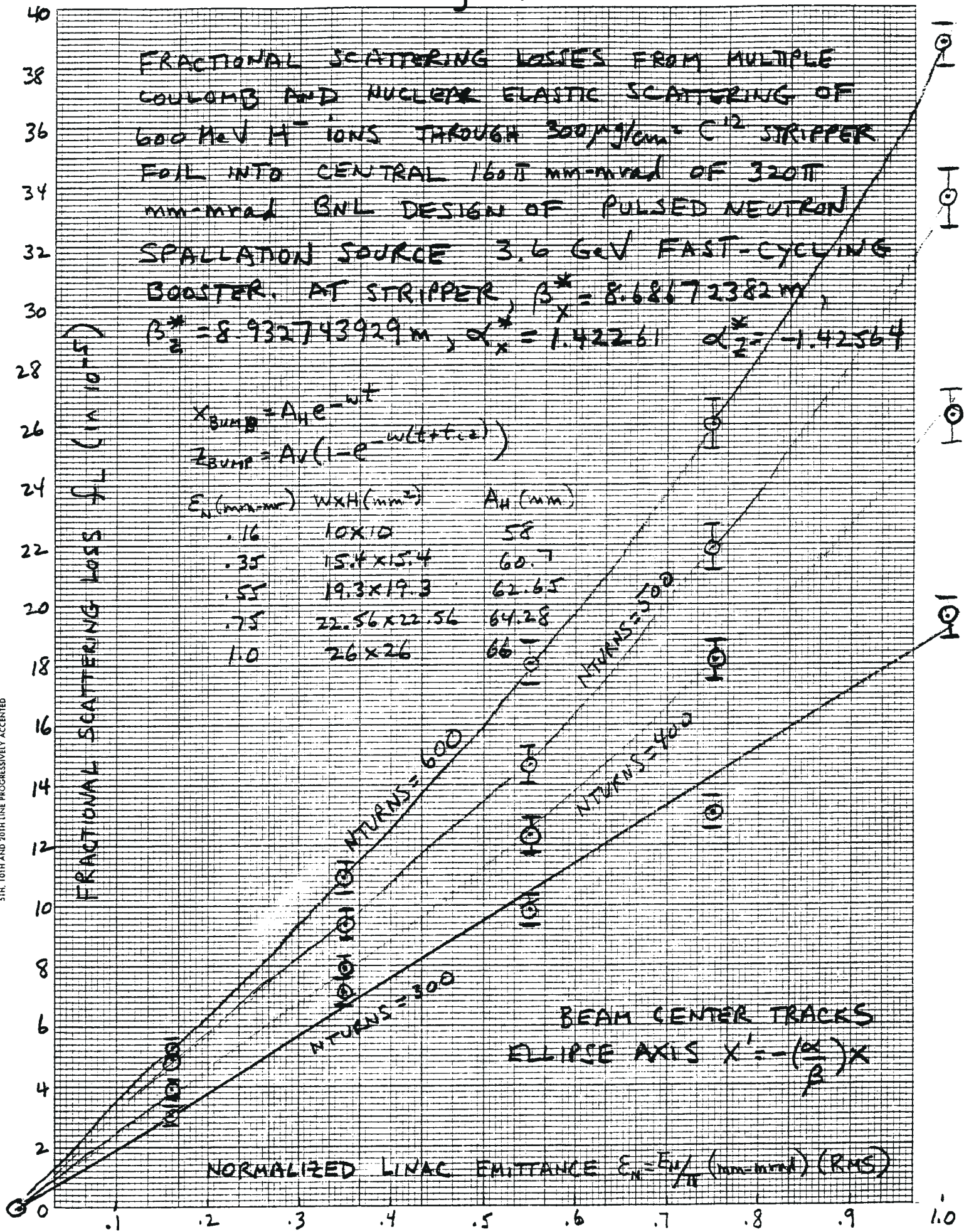


Fig. IV-3

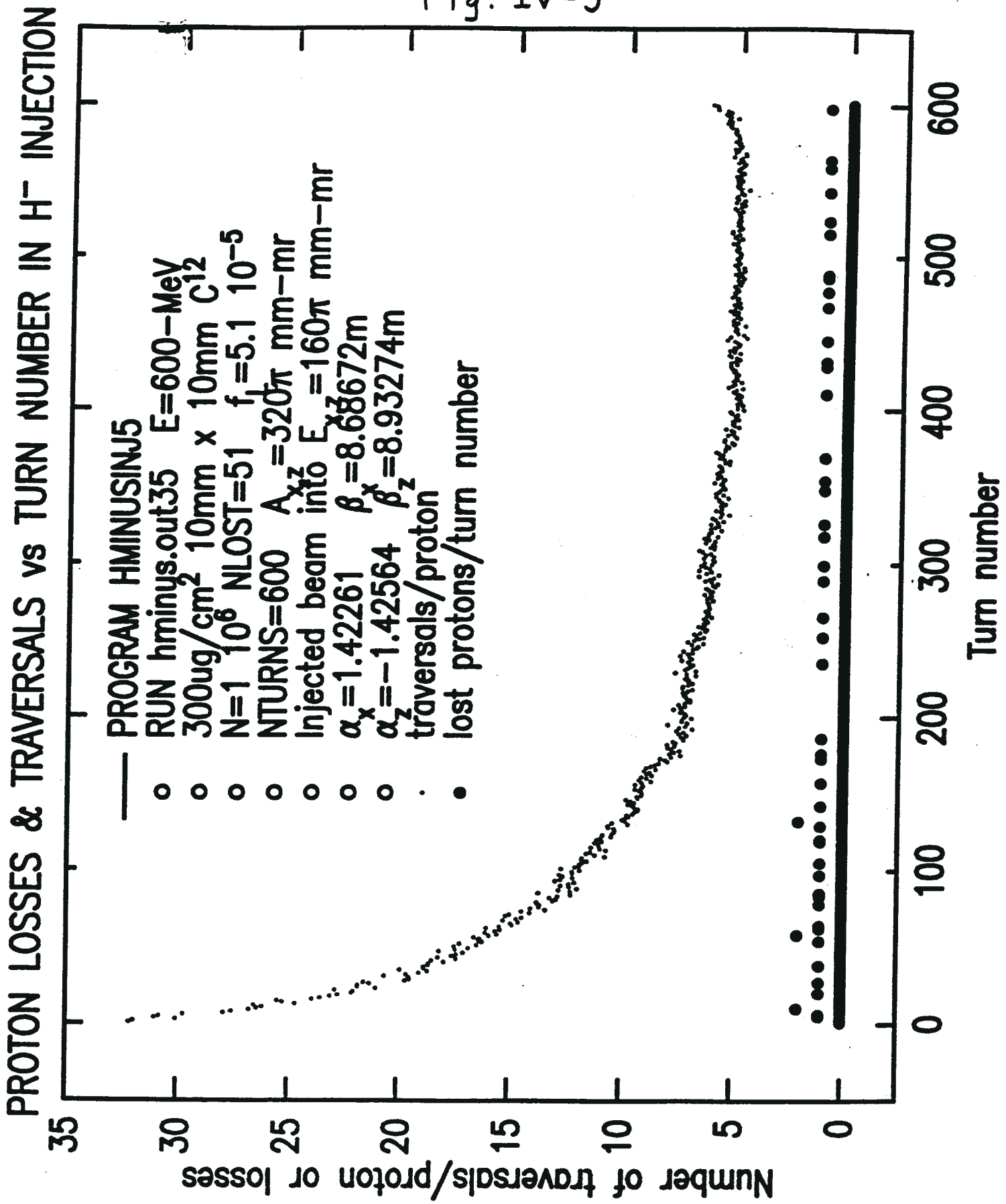


Fig. IV-4

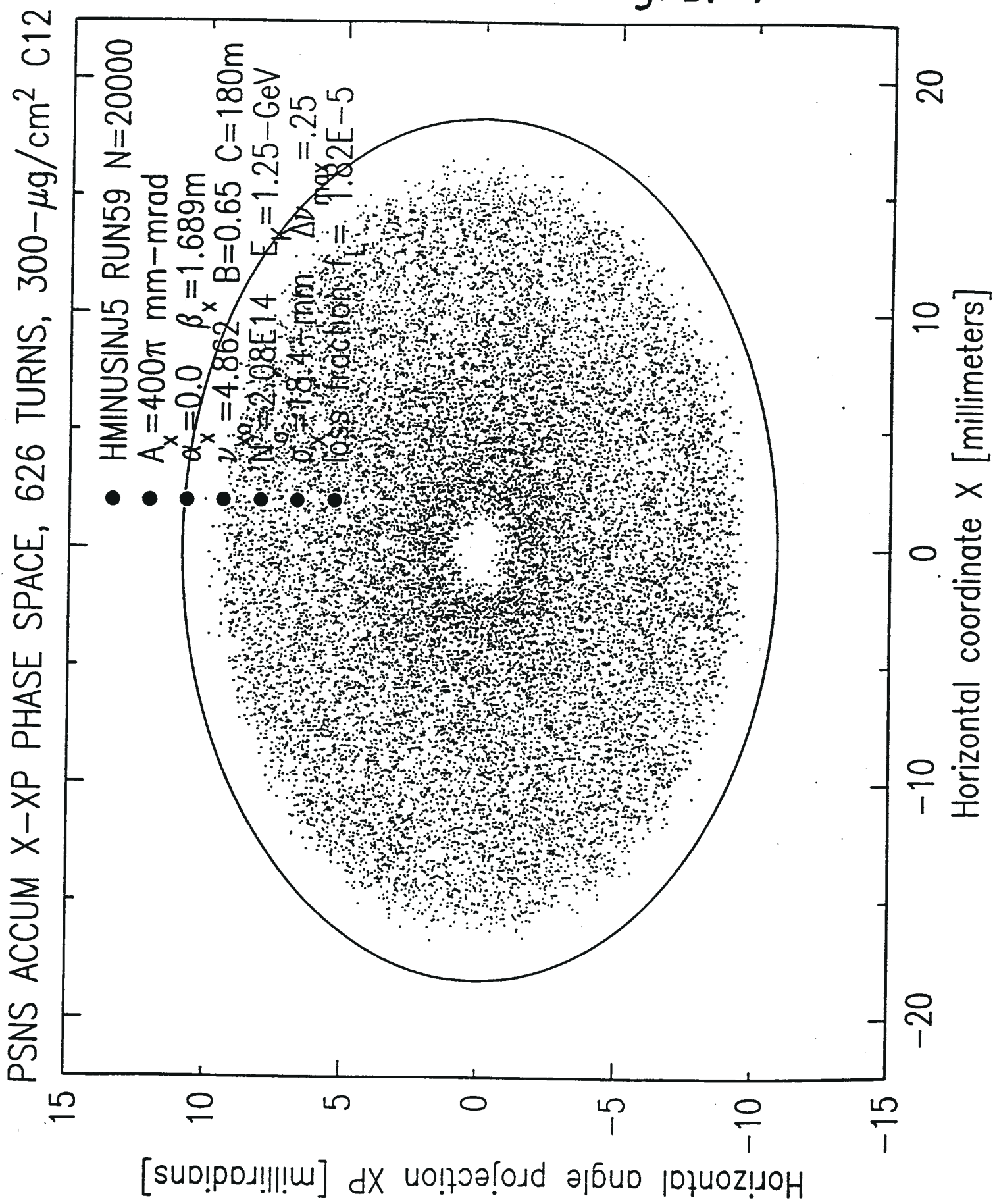


Fig. IV-5

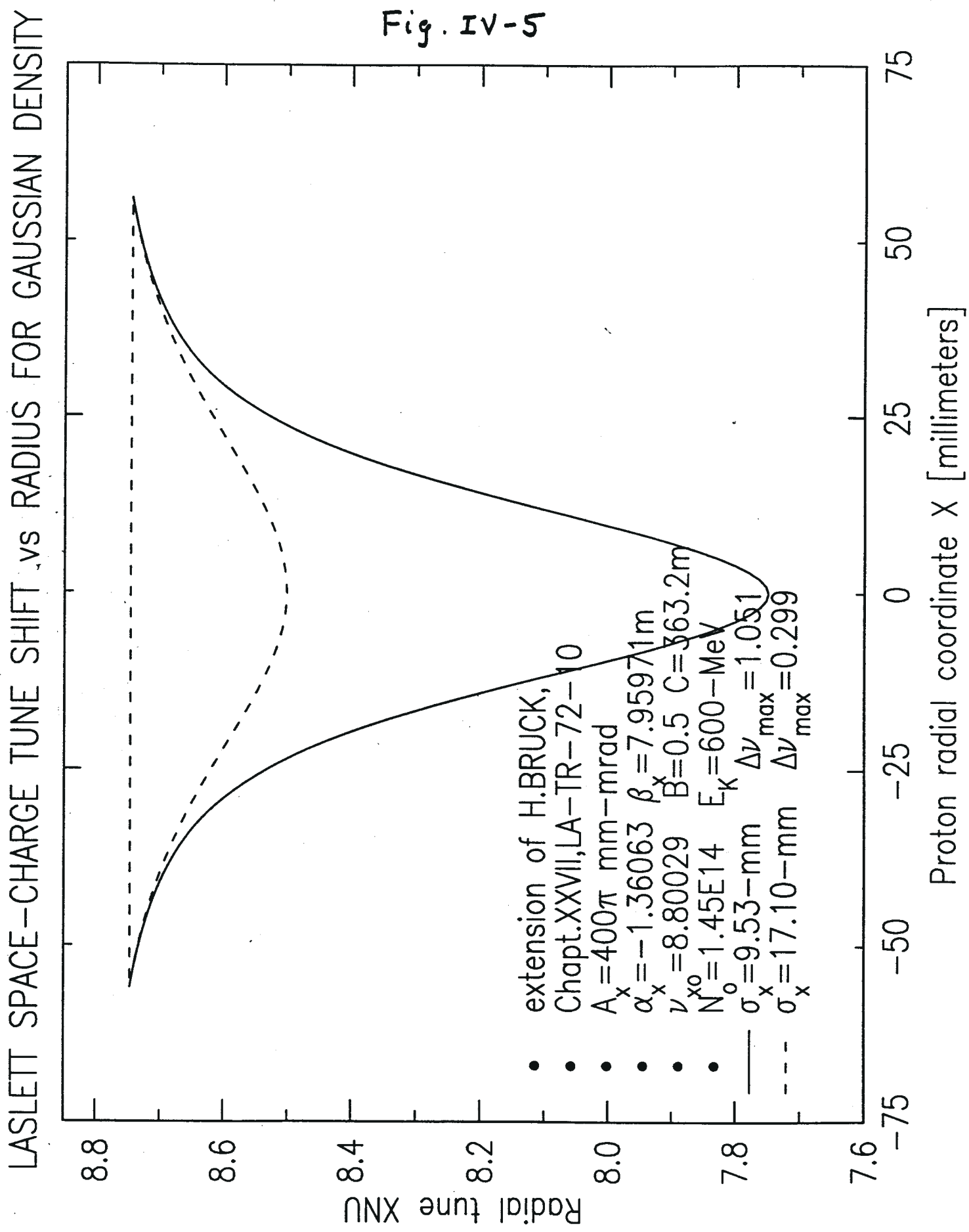
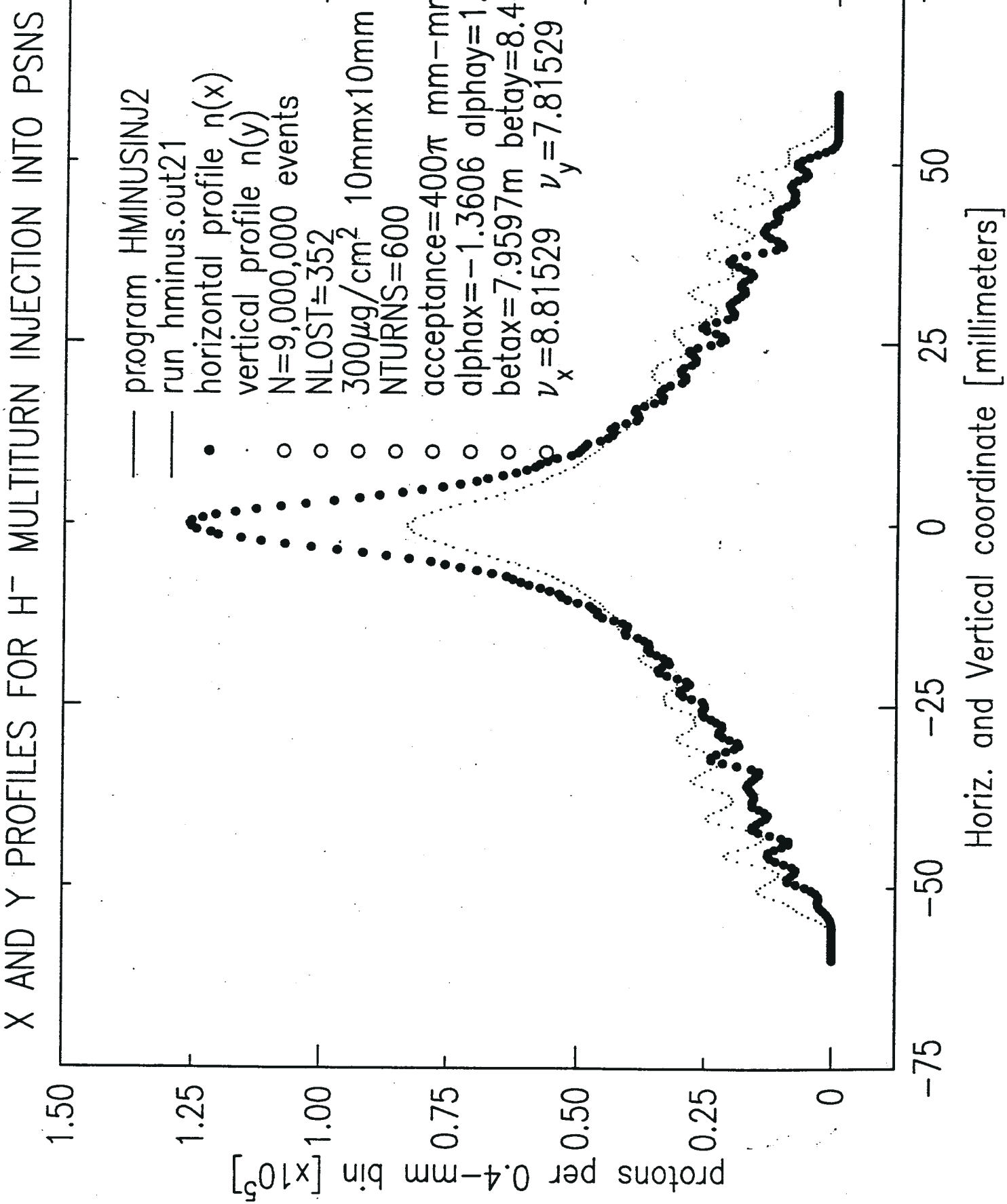


Fig. IV-6



5. Losses from Nuclear and Coulomb Interactions in the Stripper Foil.

Assuming that single particle and collective instabilities in the ring can be averted for the short storage time required in the present design, the dominant loss mechanism is removal of particles from the ring acceptance by interactions in the stripper foil. In this section we show that, at 1 GeV, the total number of nuclear interactions given by σ_T as described in Equation 4.1 is an accurate estimate of total losses. Use of a low-Z carbon stripper foil results in negligible multiple Coulomb scattering losses, and low atomic weight A minimizes nuclear losses.

Nuclear elastic scattering (NES) of 1 GeV protons on carbon has been measured by Palevsky, et al.[4.3] and their results are reproduced here as Figure V-1. Their optical model fit extrapolated to $\theta_{cm} = 0^\circ$ gives the center-of-mass differential cross section $(d\sigma/d\Omega) \approx 5 \text{ barns/sr}$. This value can be transformed to the lab system using the relativistic transformation[5.1] of solid angle from the lab to CM system. The kinematics are tabulated in Appendix C.

$$J_3 = (\Delta\Omega)_{1_{ab}} / (\Delta\Omega)_{cm} = 0.7386 \quad (5.1)$$

The program which computed the kinematics and gives the value of Equation 5.1 is TSTELKIN in Appendix B. The 0° lab cross section is then $(d\sigma/d\Omega)_L \approx 6.770 \text{ b/sr}$. The solid angle increment contained within a scattering angle θ is

$$\Delta\Omega = 2\pi(1 - \cos\theta) \approx \pi\theta^2 \quad (5.2)$$

To obtain the maximum scattering angle for which the proton can still remain within the ring acceptance, we use the half-angle of the acceptance ellipse at $x = 0$ which is given by

$$x'(x=0) = \sqrt{\epsilon/\beta_x} = 4.563 \text{ mrad} \quad (5.3)$$

where the acceptance is given for the present lattice [1.1] as $A_x = A_z = \pi\epsilon = 470 \pi \text{ mm-mrad}$ and the beta function is $\beta_x = 22.57 \text{ m}$ and $\beta_z = 5.29 \text{ m}$ at the stripper. The vertical half-angle is $z'(z=0) = 9.426 \text{ mrad}$. To obtain an estimate of the forward solid angle increment we use an average of the horizontal and vertical ellipse angles as $\bar{\theta} = 6.994 \text{ mrad}$. Then, from Equation 5.2, $\Delta\Omega = 1.537 \cdot 10^{-4} \text{ sr}$. The cross section within this solid angle is then $\Delta\sigma_e = 1.04 \text{ mb}$. The elastic, non-elastic and total cross sections have been measured by Igo, et al.[5.2] as $\sigma_e = 112 \text{ mb}$, $\sigma_{ne} = 258 \text{ mb}$ and $\sigma_T = 370 \text{ mb}$, respectively. Using their value for σ_e we see that the fraction of elastically scattered beam which remains within the machine is only 0.93%. Even a factor of two increase in the angle acceptance of the ring would not result in a significant fraction of the scattered beam remaining within the ring. At higher energy, the fraction scattered within the acceptance will be more significant since a comparison of the Palevsky data with lower energy data of Jones[5.3] given in Figure V-2 shows a significant increase in the forward CM cross section from 600 MeV to 1 GeV, together with a significant decrease in angle of the first minimum. This, together with the increased forward peaking from the CM to lab kinematic transformation and the CM to lab angle transformation will result in larger acceptance of the scattered beam than given above at 1 GeV.

Moreover, losses from multiple Coulomb scattering (MCS) become less significant at higher energy. We have evaluated MCS using Moliere's formulation[5.4] as elucidated by Bethe and Ashkin (BA)[5.5]. In Moliere's approach, the probability of scattering into an angle between θ and $\theta + d\theta$ is given by the series expansion ($\delta \equiv \theta / \theta_{mcs}$)

$$P(\delta) d\delta = \delta d\delta \left[2e^{-\delta^2} + \sum_{n=1}^{\infty} f_n(\delta) / B^n \right] \quad (5.4)$$

in inverse powers of the parameter B given by the transcendental equation

$$B - 1n(B) = b \quad (5.5)$$

The quantity b is given by BA as

$$b = 1n(\theta_i/\theta_a)^2 + 1 - 2C \quad (5.6)$$

with C = Euler's constant = 0.5772156649.... The quantity (θ_i/θ_a) in Equation 5.6 is given by BA in practical units with τ in $\mu\text{g}/\text{cm}^2$

$$\left(\frac{\theta_i}{\theta_a} \right)^2 = \frac{8.838530658 \cdot 10^{-3} (Z + 1) Z^{1/3} z^2 \tau}{\beta^2 A (1.13 + 3.76 \alpha^2)} \quad (5.7)$$

with $3.76 \alpha^2 = 2.002251163 \cdot 10^{-4} z^2 Z^2 / \beta^2$. In practical units BA gives θ_i as

$$\theta_i^2 = \frac{1.569149936 \cdot 10^{-13} Z(Z + 1) z^2 \tau}{P^2 \beta^2 A} \quad (5.8)$$

with $P = pc$ = projectile momentum in GeV. The RMS multiple Coulomb scattering angle θ_{mcs} used in the definition of δ in Equation 5.4 is given by BA as

$$\theta_{mcs} = \sqrt{\langle \theta^2 \rangle} = \theta_1 \sqrt{B} \quad (5.9)$$

The functions $f_n(\delta)$ in Equation 5.4 are given by Moliere as

$$f_n(\delta) = \frac{1}{n!} \int_0^\infty y dy J_o(y\delta) e^{y^2/4} (y^2/4 \ln y^2/4)^n \quad (5.10)$$

The Monte Carlo approach used here is to prepare tables of the integrated probability $P_I(\delta)$ from Equation 5.4 as

$$P_I(\delta) = 1 - e^{-\delta^2} + \sum_{n=1}^N F_n(\delta)/B^n \quad (5.11)$$

where the $F_n(\delta)$ are definite integrals

$$F_n(\delta) = \int_0^\delta \delta f_n(\delta) d\delta \quad (5.12)$$

These tables are used by program HMININJ6, given here as Appendix A, to select random values of δ from a uniform distribution of random numbers. Some results of the calculation are illustrated in Figure V-3 for 600 MeV protons and show the marked deviation of MCS angles from the Gaussian approximation at the large angles θ of interest in the present loss calculation. Results of several runs of HMININJ6 are given in Table I.

Table I
Particle Losses in Multiturn H⁻ Injection from Program HMININJ6

| E (GeV) | N | NTURNS | τ ($\mu\text{g}/\text{cm}^2$) | W x H (mm ²) | A/ π (mm-mm) | NINT | NSCAT | NLOST | \bar{N}_t |
|------------|----------------|--------|-----------------------------------------|-----------------------------|---------------------|------|-------|-------|-------------|
| 0.6 | $4 \cdot 10^6$ | 600 | 300 | 10x10 | 400 | 211 | 69 | 148 | 7.35 |
| 1.0 | 10^7 | 1250 | 400 | 8x4 | 470 | 333 | 94 | 175 | 4.02 |
| 1.25 | 10^7 | 626 | 300 | 6x9 | 400 | 524 | 189 | 182 | 8.0 |

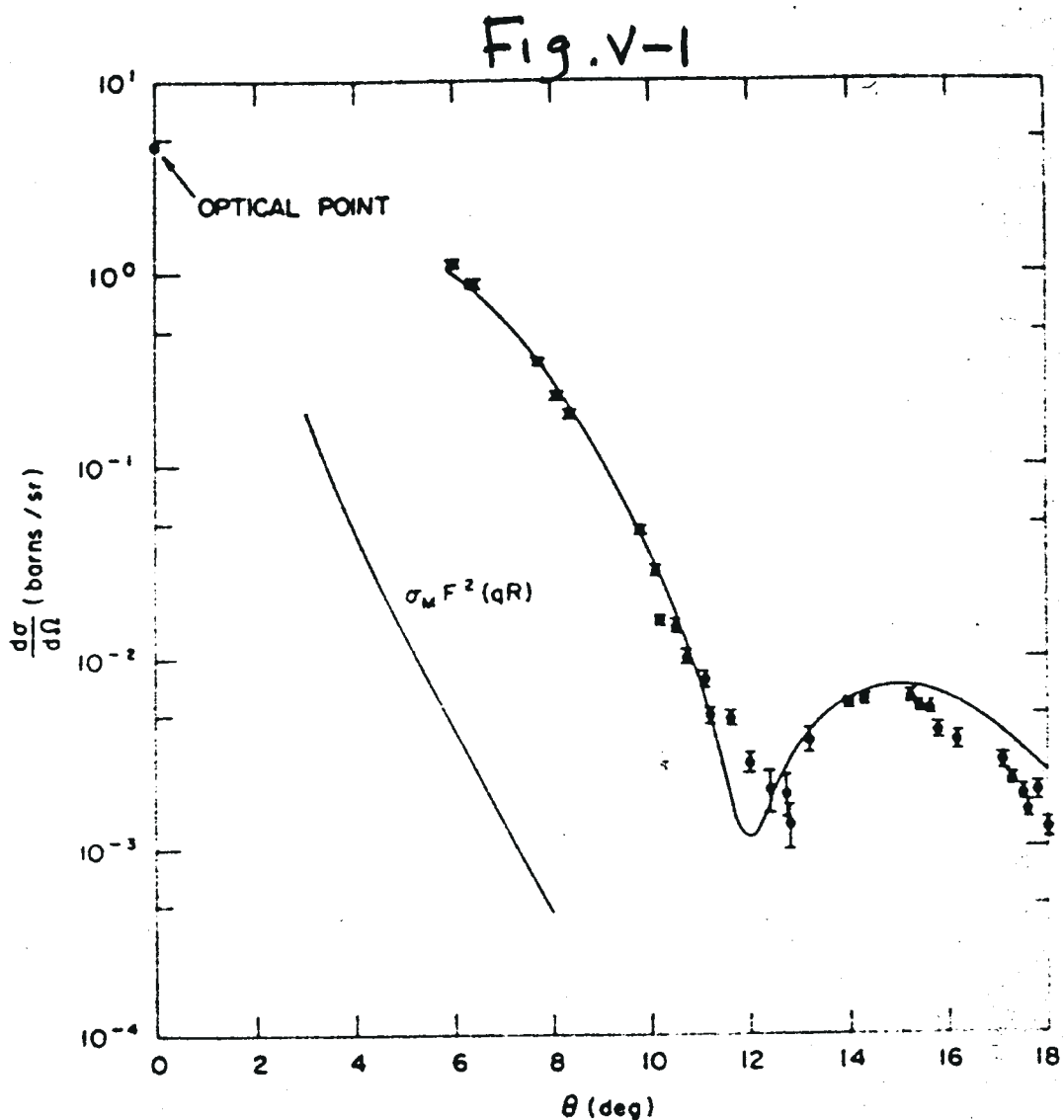
In Table I, NINT is the total number of nuclear interactions, NSCAT is the number of nuclear elastic scattering events, and NLOST is the number of particles outside of the ring acceptance A at the end of injection. At 600 MeV, we can assume from our previous discussion that essentially all of the 69 elastic scattering events are lost, and that the remaining 79 lost particles are due to multiple Coulomb scattering. Thus, MCS and NES are roughly of equal importance for losses at this energy. At 1.25 GeV, the near equality of NSCAT and NLOST indicates that losses from MCS are very small. At the intermediate energy of 1 GeV, MCS losses are only about 46% of NLOST, and thus contribute a fractional loss $f_L(\text{MCS}) \approx 8.5 \cdot 10^{-6}$. This result is consistent with the ACCSIM calculation at 1 GeV[4.2] which shows $f_L(\text{MCS}) < 10^{-4}$. For total nuclear plus Coulomb losses at 1 GeV, $NINI + (NLOST - NSCAT)$, we get $f_L = 4.32 \cdot 10^{-5}$ when account is taken of $NMISS = 421,885$ incident H⁻ ions which miss the stripper foil. It should be remarked that a higher Z, higher A stripper foil will increase both the Coulomb and nuclear losses. The nuclear total cross section is increasing rapidly with A from the Igo, et al. data[5.2].

References

- 5.1 L. Blumberg and S.I. Schlesinger, Kinematics of the Relativistic Two-Body Problem. Los Alamos Report LAMS-1718 (1955).
- 5.2 G.J. Igo, J.L. Friedes, H. Palevsky, R. Sutter, G. Bennett, W.D. Simpson, D.M. Corley and R.L. Stearns. Measurement of 1 GeV Proton Total Scattering Cross

Section on H, He, Li-6, C, O and Pb Targets. Nucl. Phys. B3 (1967), 181.

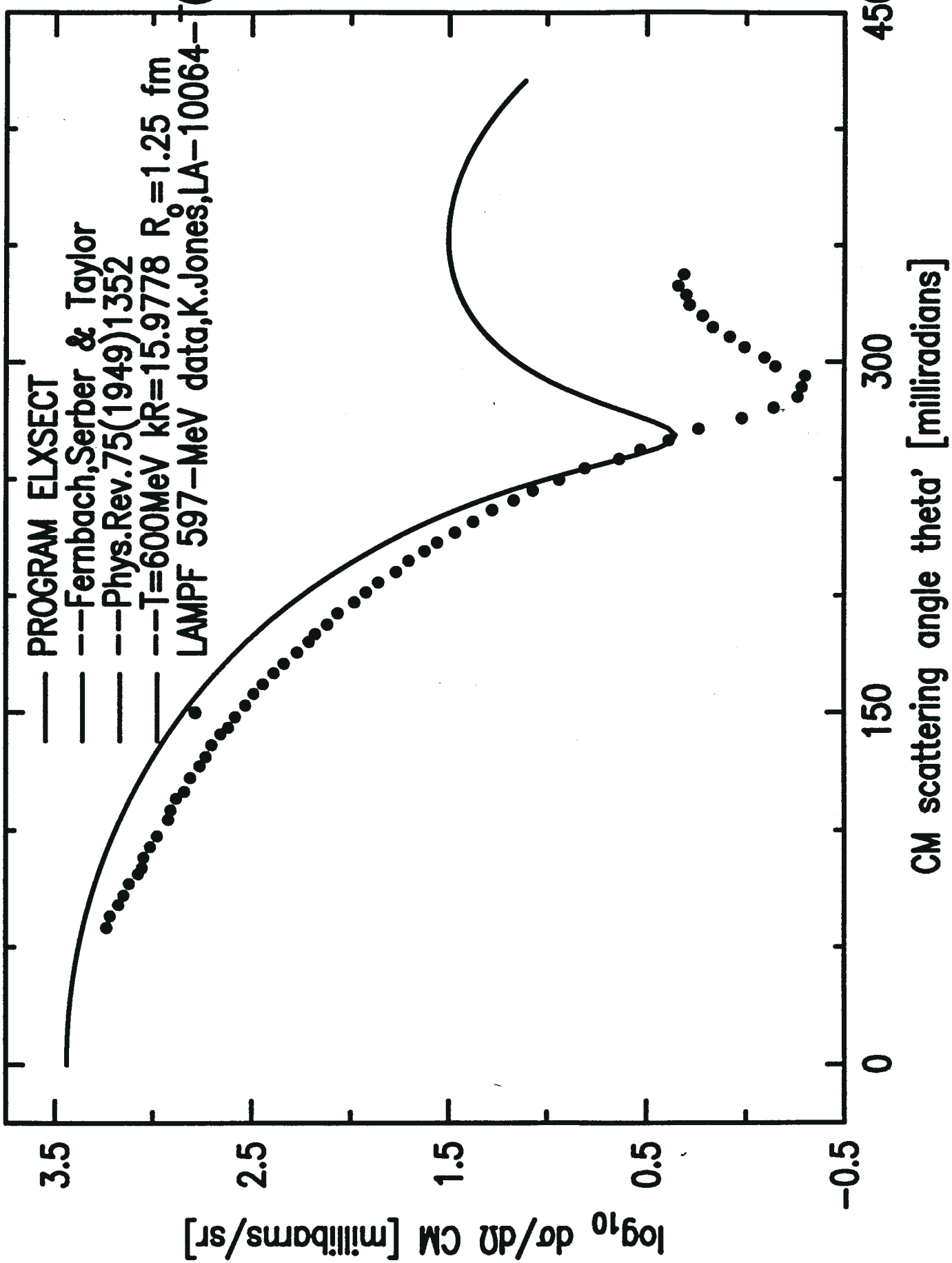
- i.3 K. Jones, Los Alamos Report LA-10064-T (1982) and private communication (1994). Dr. Jones also measured the angular distribution of p+C at 700 and 800 MeV.
- i.4 Von G. Moliere, Theorie der Streuung schneller geladenen Telchen II. Mehrfach- und Vielfachstreuung. Z. Naturforschg. 3a, 78 (1948).
- i.5 H.A. Bethe and J. Ashkin, Passage of Radiations through Matter, in Experimental Nuclear Physics, Vol. 1, Part II. E. Segré, Editor, John Wiley & Sons, Inc. (1953), pp. 166-357.



1-BeV proton elastic scattering from ^{12}C , in the center-of-mass system. The solid line is an optical-model fit to the data using a Saxon-Woods potential with the parameters given in the text. The calculated total cross section is 357 mb, in agreement with the measured value of 370 ± 9 mb.

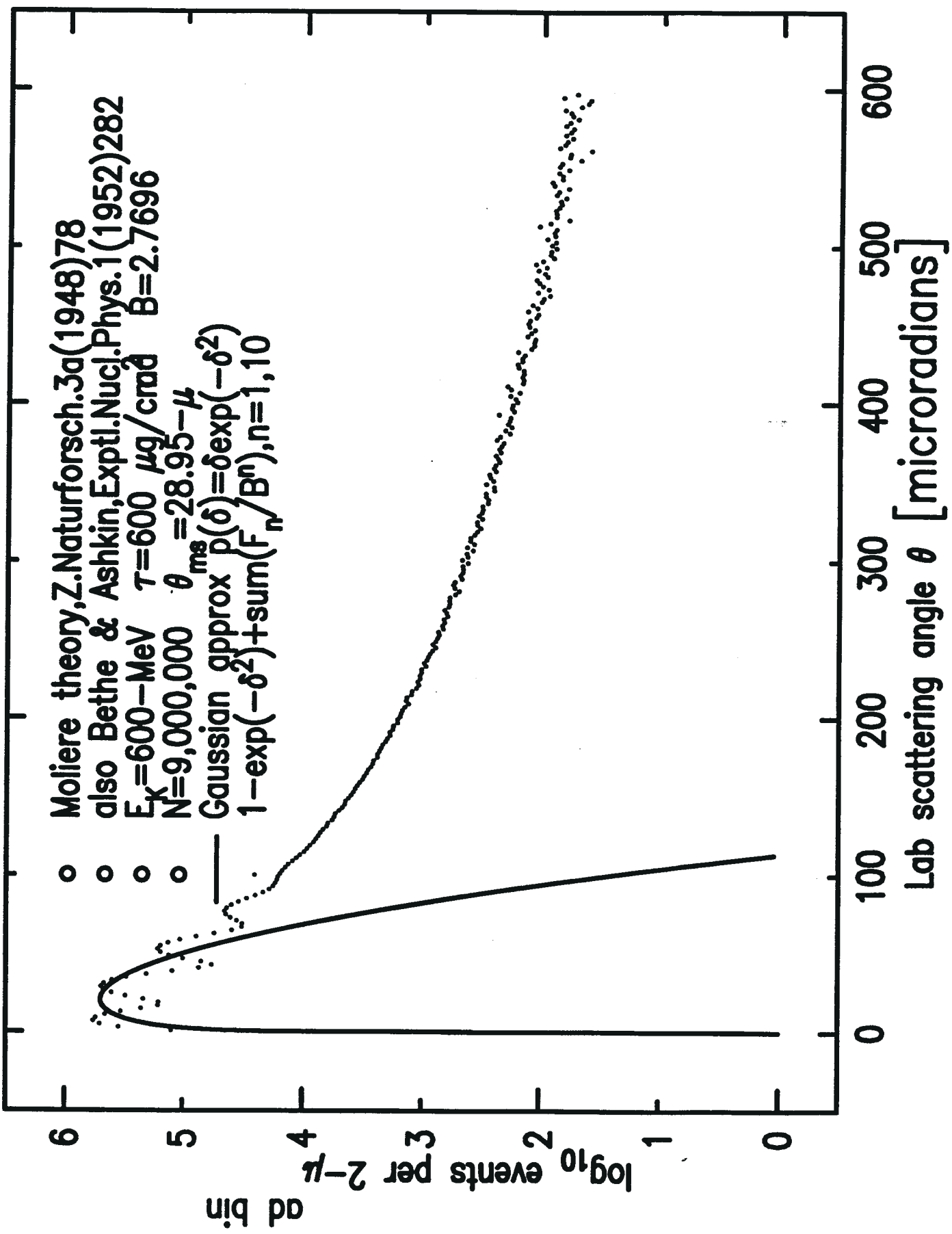
Fig. V-2

ELASTIC DIFFERENTIAL CROSS SECTION(CM), PROTONS + C₁₂



RANDOM ANGLES, MULTIPLE COULOMB SCATTERING DISTRIBUTION, P+C12

- 36 -
Fig. V-3



6. Ionization of Atomic Hydrogen in a Magnetic Field.

A fraction of the H^- beam incident on a stripper foil emerges as neutral hydrogen atoms in both the ground state and excited states. As noted in Section 3 for our $400 \mu g/cm^2$ C^{12} foil, the fraction is

$$f(H^\circ) = 1 - f_c = 1.58 \cdot 10^{-3} \quad (6.1)$$

where f_c is the fraction converted to H^+ from Equation 3.1. The number of H^- ions surviving as H^- is negligible. The H° beam then traverses dipole magnet B_3 with a fixed field of $B = 2.364$ kG, an arbitrary value chosen for convenience in the present analysis. The electric field in the H° rest frame is given by the Lorentz transformation as noted in Equation 2.2 (in MKS units)

$$E = \beta \gamma c B \quad (6.2)$$

In Figure VI-1 it is seen that excited states of H° with $n > 4$ are above the potential barrier created by the E field from a 3 kG magnetic field. However, in the rest frame of the atom, an electric field perturbs the energy levels of excited states, removing the degeneracy present at zero field. The splitting of the energy levels is the well-known Stark Effect. A lucid review of the quantum mechanical analysis of this effect can be found in Bethe and Salpeter's book[6.1]. For present purposes, the lifetimes of the states are of primary interest and we follow the analysis of Damburg and Kolosov (DK)[6.2] who give a semi-empirical expression for the width Γ of a Stark state as

$$\Gamma \approx \frac{(4R)^{2n_2 + m + 1}}{n^3 n_2! (n_2 + m)!} \exp \left[-\frac{2}{3} R - \frac{n^3 E}{4} \left(34n_2^2 + 34n_2m + 46n_2 + 7m^2 + 23m + \frac{53}{3} \right) \right] \quad (6.3)$$

In Equation 6.3 the parabolic quantum number n_2 is related to the principal quantum number n , the parabolic quantum number n_1 , and the magnetic quantum number m by [6.3]

$$n = n_1 + n_2 + m + 1 \quad (6.4)$$

and $R = (-2U_o)^{3/2}/E$ with the energy U_o of the Stark state given to 5th order in the field by DK Equation 40. In Equation 6.3, the field and energy are in atomic units with 1 a.u. of field = $5.142 \cdot 10^9$ V/cm and 1 a.u. of energy = $4.359 \cdot 10^{-11}$ ergs. The proper lifetime of the state τ_o is related to the width by the uncertainty relation $\tau_o = \hbar/\Gamma$. We assume here that the probability of radiative decay to lower-lying states is negligible compared to ionization of the atom. The European Spallation Source Group have evaluated τ vs. B for their 1.334 GeV energy[6.4] and we reproduce their results as Figure VI-2 together with a conversion of their magnetic field values and lab lifetimes τ to our 1 GeV beam energy. Similar results to those reported by the ESS Group were obtained by the Los Alamos Spallation Source Group[6.5]. Numerical checks using Equation 6.3 and DK Equation 40 are in reasonable agreement with the ESS results.

From Figure VI-2 we note, as did the ESS and Los Alamos Groups, that there is a four-order of magnitude gap between the least bound $n = 4$ state and most-bound $n = 5$ state. For states more strongly bound than the least-bound state of $n = 4$, the lifetimes are $>> 10^7$ sec and for the states less strongly bound than the most-bound state of $n = 5$, the lifetimes are $<< 10^{-11}$ sec. We assume for the present upper limit estimate of ionization losses that all H° 's in the $n = 4$ and $n = 5$ states are in these limiting Stark levels. An estimate of the population of these excited states is more difficult since the experimental evidence on population of excited H° states following H^- traversal of thin carbon foils appears to give a population dependence on foil thickness. Mohagheghi, et al.[6.6] report measurements of population of $n = 2$ to 5 states for 800 MeV H^- and parameterize their results in a power law distribution $N(n) \sim 1/n^p$ with p decreasing from 3.54 to 1.29 as foil thickness increases from 19 to $198 \mu\text{g}/\text{cm}^2$. Extrapolating their results to our $400 \mu\text{g}/\text{cm}^2$ foil seems inappropriate.

The parameter p also depends on H^- beam energy. Their results for $n = 10$ and 11 states at 800 MeV show $p \approx 8$ over a wide range of foil thicknesses up to $300 \mu g/cm^2$. Los Alamos suggests a $1/n^2$ dependence[6.7] and we adopt that value for our present estimate. The population of the excited states from the Los Alamos distribution is given in Table I. The relative abundance of $n = 4$ is $3.8 \cdot 10^{-2}$ and of $n = 5$ is $2.43 \cdot 10^{-2}$. Using Equation 6.1 for the H° fraction of the incident H^- beam, the fractions of the original H^- beam in $n = 4$ and $n = 5$ are then $6.00 \cdot 10^{-5}$ and $3.84 \cdot 10^{-5}$, respectively.

Table I
Population of Excited States of H° from $1/n^2$ Distribution

| n | $1/n^2$ | $\sum_n^\infty 1/n^2$ | $1/n^2 / \sum_{n=1}^\infty 1/n^2$ | $\sum_n^\infty 1/n^2 / \sum_{n=1}^\infty 1/n^2$ |
|-----|---------|-----------------------|-----------------------------------|-------------------------------------------------|
| 1 | 1.0 | 1.644725 | 0.6080 | 1.0 |
| 2 | 0.25 | 0.644785 | 0.1520 | 0.3920 |
| 3 | 0.1111 | 0.394830 | 0.0675 | 0.2401 |
| 4 | 0.0625 | 0.283719 | 0.0380 | 0.1725 |
| 5 | 0.0400 | 0.221249 | 0.0243 | 0.1345 |
| 6 | 0.0278 | 0.181249 | 0.0169 | 0.1102 |
| 7 | 0.0204 | 0.153471 | 0.0124 | 0.0933 |
| 8 | 0.0156 | 0.133063 | 0.0095 | 0.0809 |
| 9 | 0.0123 | 0.117460 | 0.0075 | 0.0714 |
| 10 | 0.0100 | 0.105114 | 0.0061 | 0.0639 |

It is clear from the above discussion that magnetically stripped H° 's from the $n = 4$ and 5 states cannot contribute losses exceeding our criterion of $< 10^{-4}$ for uncontrolled loss. It is worthwhile, however, to examine these losses further. For the $n = 4$ states with assumed

lifetime $\tau = 0.85 \cdot 10^{-7}$ sec, the stripping length in magnet B_3 is

$$\lambda_s = \beta c \tau = 22.3 m \quad (6.5)$$

The fraction of these H° 's that strip to protons in the $L = 0.8$ m length of B_3 is then $f_L = 1 - \exp(-L/\lambda_s) \approx L/\lambda_s = 0.0359$. This loss represents $2.15 \cdot 10^{-6}$ of the incident H^- beam and is thus negligible. For the H° 's in the $n = 5$ state with an assumed lifetime of $\tau = 0.85 \cdot 10^{-11}$ sec, we note first that losses will result if the stripping occurs at a point in the dipole such that the deficit in bend angle of the resulting proton exceeds the angle acceptance of the ring. The average angle change needed to remove a proton is approximately the half-width of the ellipse in the x' direction, i.e., $\Delta x' = x' (x = 0) = \sqrt{\epsilon/\beta}$. Using the acceptance of $\epsilon = 470$ mm-mrad and the beta function at the foil of $\beta = 22.57$ m which is close to the beta value at the upstream end of B_3 , we get $\Delta x' = 4.56$ mrad. This angle is 0.136 of the 33.43 mrad bend of B_3 and, if we assume a sharp cut-off field for the dipole, represents a distance of $d = 10.88$ cm of the 80 cm magnet length. We can compute the stripping length for H° 's of lifetime $\tau = 0.85 \cdot 10^{-11}$ sec by using Equation 6.5 to get $\lambda_s = 2.23$ mm. The fraction of H° 's which remain in the beam after traversing length d is then $f(d) = \exp(-d/\lambda_s) \approx 0$. Thus, protons resulting from ionization of the $n = 5$ state remain within the ring acceptance.

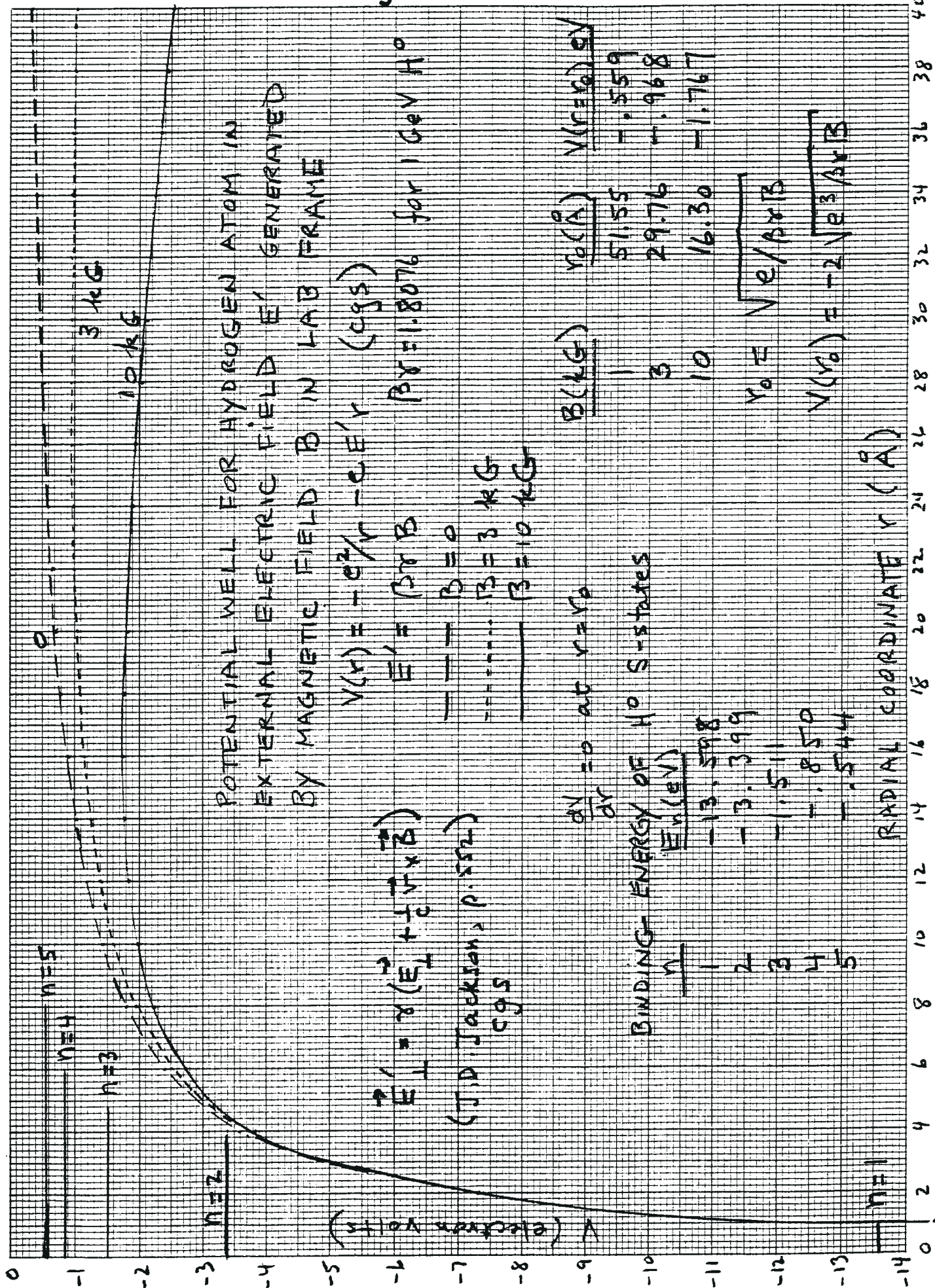
In summary, we have shown that essentially all of the H° 's in states $n \geq 4$ survive traversal through B_3 whereas essentially all H° 's in states $n > 5$ are stripped but remain within the acceptance. The fraction of H° 's with $n \geq 4$ is, from Table I, $f(n \geq 4) = 0.8655$ and thus the fraction of the original H^- beam transmitted as H° 's through B_3 is $f(H^\circ) = 1.367 \cdot 10^{-3}$. There are several methods to dispose of this H° beam: (1) convert them to H^+ in a second stripper foil downstream of B_3 and bend the protons out of the ring with a septum magnet, (2) let the H° 's go through the aperture of the downstream quadrupole QD and convert them to protons in the next half-cell of the lattice, or (3) stop the H° 's in a beam dump within the injection straight section as indicated in Figure I-1. We believe that

this controlled loss is acceptable since the beam dump can be removed remotely if maintenance on the magnets or stripper foil changing mechanism is required. The nuclear interaction length in a heavy metal such as tungsten is 185 g/cm^2 [6.8] and, with a density of 19.3 g/cm^3 , $\lambda_{\text{int}} \approx 9.6 \text{ cm}$. We could easily accommodate a dump of length $10 \lambda_{\text{int}}$ which, as seen from Figure VI-3, is about 3 times the range of 1 GeV protons.

References

- 6.1 H.A. Bethe and E.E. Salpeter, Quantum Mechanics of One-and Two-Electron Atoms. Plenum Publishing Corp. (1977), Sect. 51, p. 228.
- 6.2 R.J. Damburg and V.V. Kolosov, Theoretical Studies of Hydrogen Rydberg Atoms in Electric Fields, Chapt. 2 in Rydberg States of Atoms and Molecules. R.F. Stebbings and F.B. Dunning, Editors, Cambridge University Press (1983).
- 6.3 Ibid, Ref. 6.1, Sect. 6, p. 27.
- 6.4 Outline Design of Rings for a European Spallation Neutron Source, Rings' Working Group Report, ESS 94-14-R (December, 1994).
- 6.5 Preliminary draft of Los Alamos proposal for Next-Generation Spallation Neutron Source, Sect. 2, private communication (August, 1994).
- 6.6 A.H. Mohagheghi, H.C. Bryant, P.G. Harris, R.A. Reeder, H. Sharifian, C.Y. Tang, H. Tootoonchi, C.R. Quick, S. Cohen, W.W. Smith and J.E. Stewart, Interaction of Relativistic H^- Ions with Thin Foils, Phys. Rev. A43, 1345 (1991).
- 6.7 A.J. Jason, private communication (April, 1996).
- 6.8 Particle Data Group, Review of Particle Properties, Phys. Rev. D50, 1173 (1994).

Fig. VI-1



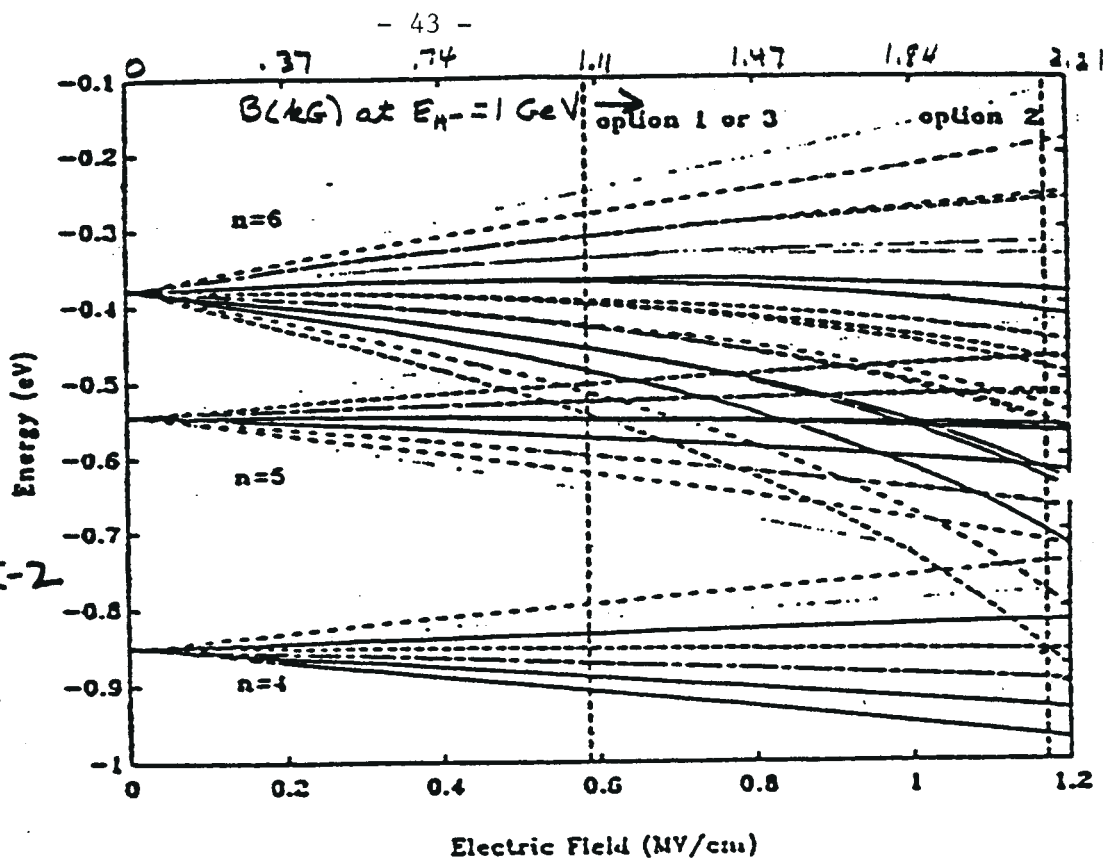


Fig. VI-2

FROM "OUTLINE DESIGN OF RINGS FOR A EUROPEAN SPALLATION NEUTRON SOURCE" ESS-94-14-R (1994)

Energy Levels of Stark States
B (kG) at $E_{H^-} = 1.0 \text{ GeV}$ →

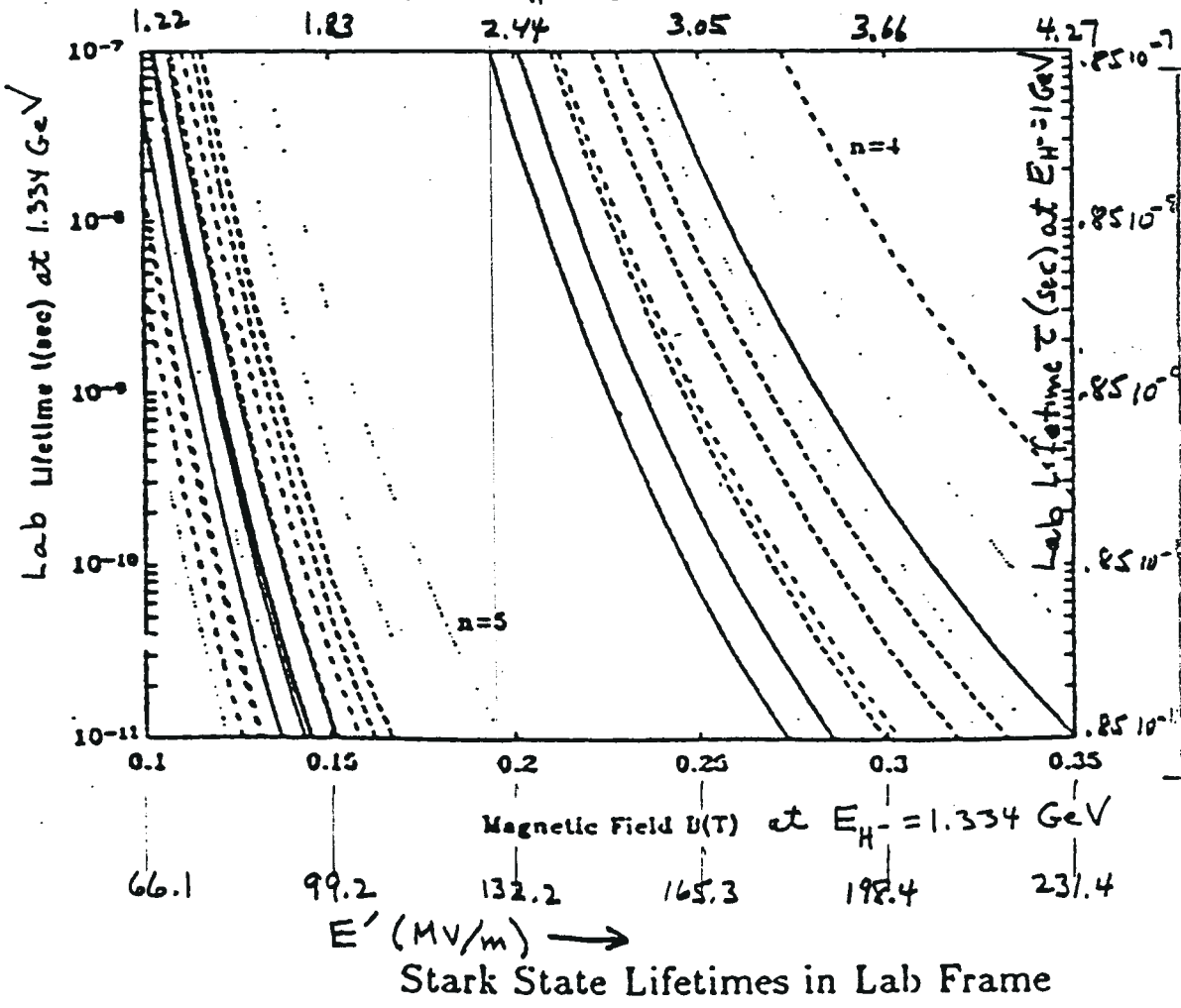
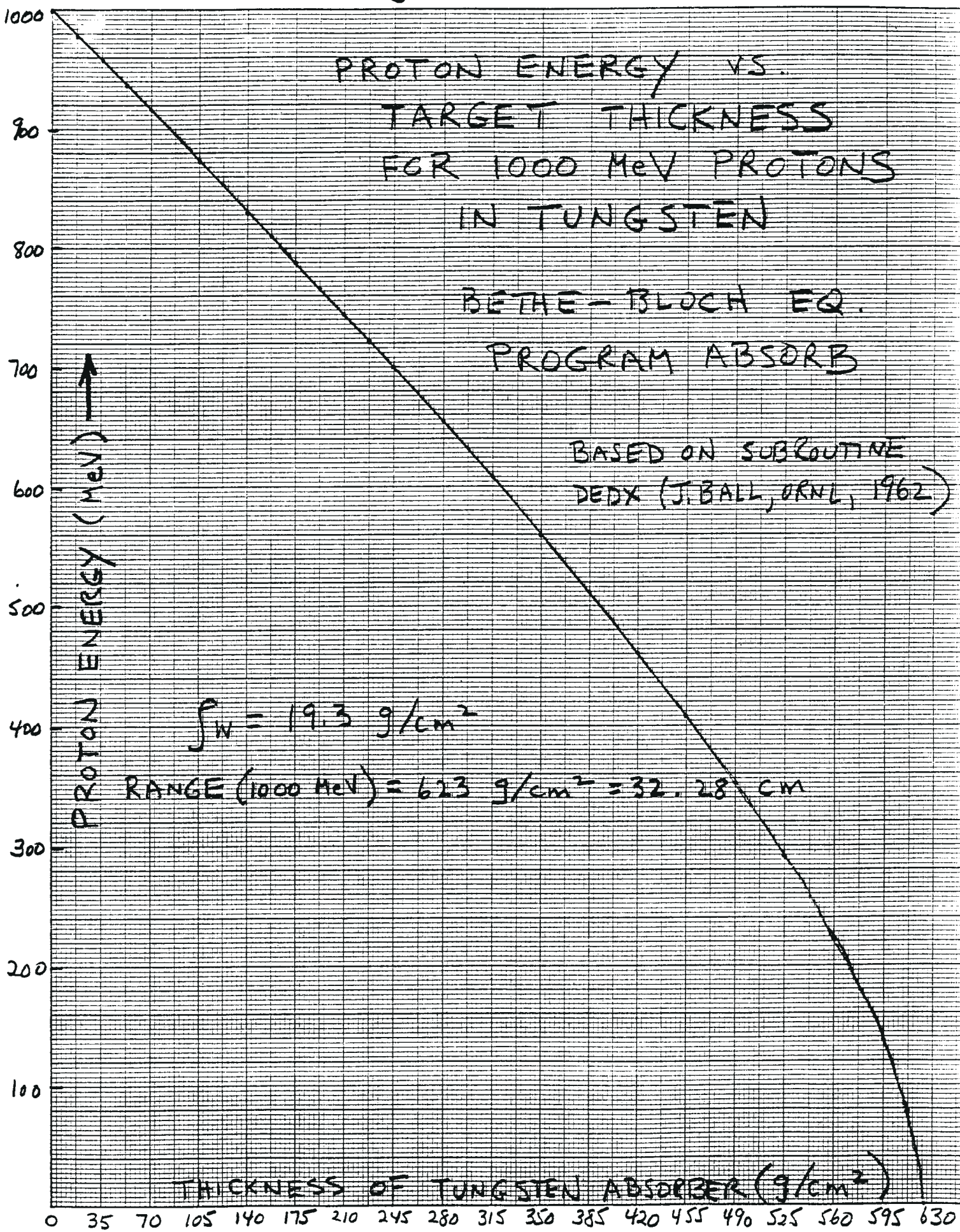


Fig. VI-3

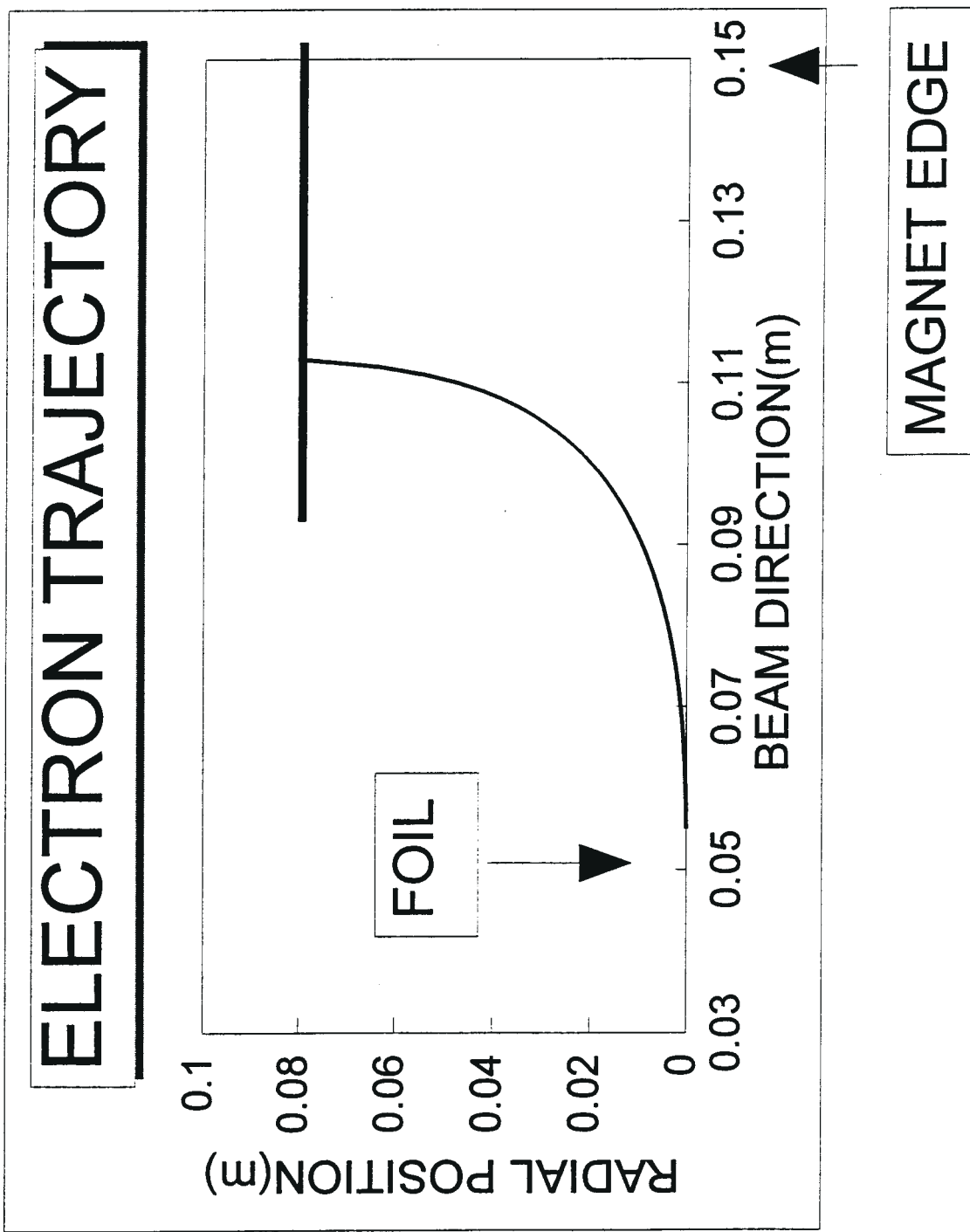


7. Electron Sweeping and Collection.

The stripped electrons from incoming H^- have a momentum of 0.923 MeV/c and a magnetic rigidity of 0.00308 T-m. The electrons travel with the protons until they encounter a magnetic field. The first magnetic field the electron encounters is the field of orbit bump dipole. The dipole has a fixed field of 0.23 T, which is to minimize the halo created by the excited states of H° . The magnetic fringe field extends to approximately a distance corresponding to its gap height. The figure shows the electron trajectory assuming linearly decreasing fringe field extending to 10 cm upstream of the magnet. The electron trajectory becomes a right angle to the proton orbit several centimeters upstream of the magnet and 8 cm outside of the orbit. We place collection plate parallel to the proton orbit at this location. The final position of the collector plate should be determined by the magnetic measurement of the dipole.

The collection plate is water cooled, as the electron power is expected to be about 1/900 of the proton power (about 1 KW for 1 MW NSNS). The collection plate will be electrically biased so that no secondary electron, generated by the stripped electron striking the plate escapes the plate. One has to minimize free electron generation for free electrons inside the ring can cause an instability to the stored protons.

Fig. VII-1



8. Foil Temperature Considerations.

Carbon foils are used to strip electrons because of resiliency and high sublimation temperature of the material. The sublimation temperature of carbon is above 3500 degrees Kelvin. The foil is heated by the energy deposited by the proton and two accompanying electrons. Since they all have the same velocity, they should have the same energy losses in a given material.

There is no date available for what fraction of the energy is lost by the beam in the material contributing toward heating of the material. At higher energies, the efficiency is estimated to be as low as 30%. However, for our calculations, we assume that all the energy loss contributes to the heating of the material. Furthermore, we assume that no heat dissipates by conduction along the foil edge and the black body radiation is the only mechanism which dissipates the heat.

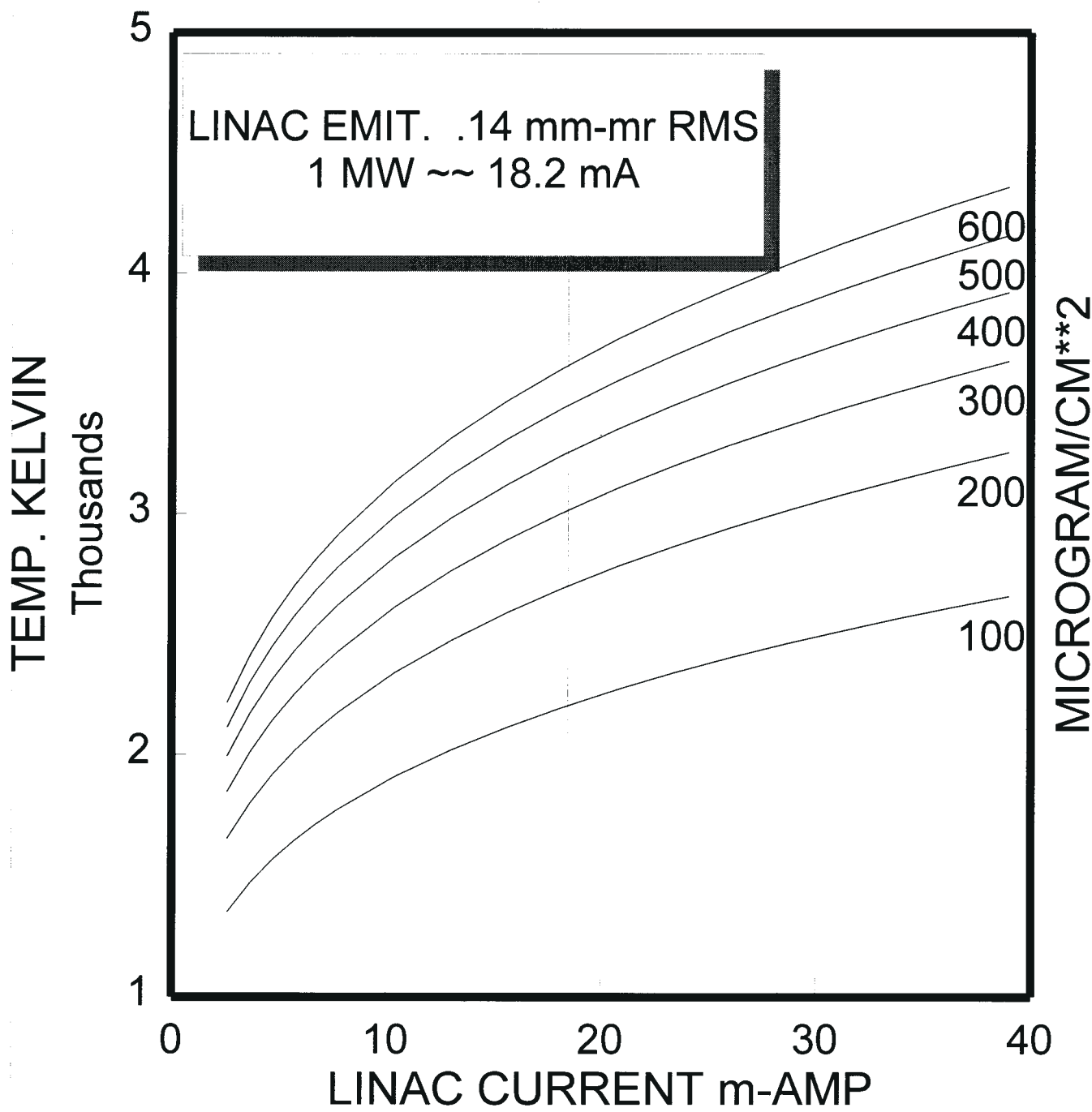
For one megawatt NSNS injection, the linac has the following parameters. The effective average current at the injection point is 18.2 milliamperes in the unnormalized RMS emittances of 0.14 mm-mr in both planes. The peak current density at the foil, where the beta-functions are 24 and 5 meters, is about 3800 A/m^2 . The temperature at the spot will rise very quickly to the equilibrium where the heat input and the black body radiation become equal. Since the heat input is proportional to the thickness of the foil while the black body radiation is proportional to the surface area, the thicker the foil, the higher the resultant equilibrium temperature. The figure shows the calculated equilibrium temperatures for effective linac current. In this calculation, we assumed the emissivity of the carbon foil to be 0.8.

For the linac current assumed for the NSNS injection, up to $400 \mu\text{-g/cm}^2$ foil can survive the injection where a thicker foil may reach sublimation temperature. In case we double the linac current for increased power, we may consider a tandem foil of two $200 \mu\text{-g/cm}^2$ about a cm apart. The foil may lose some solid angle to radiate the heat; however, they have enough solid angle to radiate and would survive the injection.

PEAK FOIL TEMP. vs LINAC H- CURR.

100% ENER. DEP. 80% EMISSIVITY

Fig. VIII-I



- 49 -
Appendix A

PROGRAM HMINUSINJ6

C Evaluates injection losses from scattering of H-minus beam of N
C particles of momentum P(GeV/c) and emittances EX and EZ(mm-mrad)
C incident on stripper foil of thickness TAU(ug/cm2), atomic number TZ,
C atomic weight TA(amu). Particles are followed around ring for NTURNS
C on a horizontally collapsing exponential orbit bump from time TI
C to TF(sec). Ring has a rotation period TR, horizontal and vertical
C tunes XNU0 and ZNU0, beta values BX and BZ(m) and admittances AX,AZ
C (mm-mrad). Subroutine MCSCAT calculates Moliere multiple coulomb(MCS)
C scattering if particle crosses foil of width W and height H(mm) and
C inner edge position XF0(mm). OMH and OMV are rate constants(1/sec) of
C horiz. and vertical exponential orbit bumps, XC=AH*exp(-(t-TI)*OMH),
C amplitude AH and AV(mm). Intermediate printout provided if INT.LT.N.
C Distribution of losses is given in LOSSTURN array & distribution of
C foil traversals in TRAVERS .Uses random generators RAND and GASDEV
C from Numerical Recipes. If NPLOT.GT.0, individual coordinates XXPZZP(J)
C written to EPFILE. Data input from INFILE. Ellipse tilted if ALFX &
C ALFZ nonzero. H-minus beam center is on line x'=-alpha*x/beta if NBC.
C NE.0 or on line x'=z'=0 if NBC.EQ.0. Initial proton chosen at random
C injection time between TI and TF and followed until bump collapses to
C zero. Nuclear elastic(NES) scattering(Fernbach,Serber,Taylor) done in
C ELSCAT from distribution function FE(I,J) via COMMON/FESTABLE in file
C FESFILE.Distribution function FM(I,J) for MCS in COMMON/FMCTABLE read
C from file FMCFILE. Space-charge shifted tunes XNU,ZNU and one-turn
C transport matrices XM,ZM calculated by subroutine TUNE. 11/13/93.
C AH = amplitude of horizontal fast bump (mm)
C ALFX=horizontal alpha function at stripper foil
C ALFZ=vertical alpha function at stripper foil
C AV = amplitude of vertical fast bump (mm)
C AX = horizontal admittance ellipse area/pi (mm-mrad)
C AZ = vertical admittance ellipse area/pi (mm-mrad)
C B = Moliere's distribution function expansion coefficient.
C BUN= Ring bunching factor
C BX = horizontal beta function at stripper foil (m)
C BZ = vertical beta function at stripper foil (m)
C C = Ring circumference (m)
C DEL= bin size in X and Y distributions (mm)
C DELP=bin size in XP and YP distributions (mrad)
C DNMX=maximum space-charge tune shift deltanux at ring center
C DNMZ=maximum space-charge tune shift deltanuz at ring center
C EPFILE=file with XXPZZP(I,J) if NPLOT.NE.0, I=1,4 J=1,N
C EX = horizontal emittance area/pi of H-minus beam (mm-mrad)
C EZ = vertical emittance area/pi of H-minus beam (mm-mrad)
C FESFILE=file with distribution function for elastic scattering
C FMCFILE=file with distribution function for mult.coul.scatt.
C FE = elastic scattering array with angle THLAB and F(THLAB)
C FM = mult.coul.scatt.array with del and Fn(del), n=1,..10
C H = vertical size (height) of stripper foil (mm)
C INFILE=name of input data file
C INT = number of pulses per intermediate results output
C N = number of injected particles
C NB = number of bins in output X,XP,Y,YP arrays
C NBC= test# for H-minus beam angle.NBC=0=no angle offset of XPB,ZPB
C NEL= number of entries desired in elastic scatt.dist. function
C NINT=number of nuclear interactions in stripper foil
C NMC= number of entries desired in Moliere distribution function
C NMIS=number of injected particles that missed stripper foil
C NPLOT=number of particle coordinates written to EPFILE
C NS = seed number for random number generator
C NT = number of terms in Moliere distribution series

C NTURNS=number of injected turns per injection pulse
C OMH= collapse rate OMEGA(1/sec) of horiz. exponential fast bump
C OMV= rise rate OMEGA(1/sec) of vertical exponential fast bump
C OUTFILE=name of file with output results
C P = momentum of incident H-minus (GeV/c)
C PROBINT=probability of nuclear interaction in stripper foil
C PROBSCAT=probability of elastic nuclear scattering in foil
C SIGD=nuclear elastic scattering total cross section (mb)
C SIGRX=rms X-width of beam charge distribution in ring (mm)
C SIGRZ=rms Z-width of beam charge distribution in ring (mm)
C SIGT=total nuclear interaction cross section in foil (mb)
C TA = atomic weight of stripper foil material (amu)
C TAU= areal density of stripper foil (ug/cm²)
C TF = start time of final injected H-minus pulse (msec)
C TI = start time of initial injected H-minus pulse (msec)
C TIZ= time off-set(msec) of vertical bump
C TR = rotation period of ring (microsec)
C TZ = atomic number of stripper foil material
C W = horizontal size (width) of stripper foil (mm)
C XF0= horizontal position of inner edge of stripper foil (mm)
C XM = one-turn horizontal transport matrix XM11,XM12,XM21,XM22
C XNO= total number of protons in ring
C XNU= horizontal ring tune at position X with space-charge
C XNU0=horizontal ring tune without space charge
C ZM = one-turn vertical transport matrix ZM11,ZM12,ZM21,ZM22
C ZNU= vertical ring tune at position Z with space-charge
C ZNU0=vertical ring tune without space charge
IMPLICIT REAL*8 (A-H,O-Z)
INTEGER*4 NS
CHARACTER*10 DAY,HOUR
CHARACTER*12 EPFILE,FESFILE,FMCFILE,INFILE,OUTFILE
CHARACTER*80 HEADER
DIMENSION X(900),NX(900),TX(900),NTX(900),Y(900),NY(900),TY(900),
1 NTY(900),XXPZZP(4),LOSSTURN(999),TRAVERS(999),XM(4),ZM(4)
COMMON/FESTABLE/FE(2,901)
COMMON/FCMCTABLE/FM(11,1500)
COMMON/TUNEDAT/ALFX,ALFZ,BUN,BX,BZ,C,DNMX,DNMZ,AX,AZ,PM,P,SIGRX,
1 SIGRZ,XNO,XNU0,ZNU0
TWOP=6.283185307179586D0
PM=.93827231D0
CALL DATE(DAY)
CALL TIME(HOUR)
C read input data
WRITE(*,*) ' enter name of input data file INFILE(A12)='
READ(*,*) INFILE
OPEN(13,FILE=INFILE,STATUS='OLD',FORM='FORMATTED')
C WRITE(*,*) ' enter HEADER(A80)='
READ(13,*) HEADER
C WRITE(*,*) 'enter N,NS,NEL,NMC,NT,NTURNS,NB,INT,NPLOT,DEL,DELP='
READ(13,*) N,NS,NEL,NMC,NT,NTURNS,NB,INT,NPLOT,DEL,DELP
C WRITE(*,*) 'enter P,TA,TAU,TZ,EX,EZ,W,H,XF0,SIGD,SIGT,NBC='
READ(13,*) P,TA,TAU,TZ,EX,EZ,W,H,XF0,SIGD,SIGT,NBC
C WRITE(*,*) ' enter XNU0,ZNU0,AX,AZ,BX,BZ,TR,OMH='
READ(13,*) XNU0,ZNU0,AX,AZ,BX,BZ,TR,OMH
C WRITE(*,*) ' enter OMV,AH,AV,TI,TF,TIZ,ALFX,ALFZ='
READ(13,*) OMV,AH,AV,TI,TF,TIZ,ALFX,ALFZ
C WRITE(*,*) ' enter BUN,C,DNMX,DNMZ,SIGRX,SIGRZ,XNO
READ(13,*) BUN,C,DNMX,DNMZ,SIGRX,SIGRZ,XNO
C WRITE(*,*) 'enter names files FESFILE,FMCFILE,OUTFILE='
READ(13,*) FESFILE,FMCFILE,OUTFILE

```

IF(NPLOT.GT.0) THEN
  WRITE(*,*) 'enter name of phase space plot file EPFILE(A12)='
  READ(13,*) EPFILE
  OPEN(12, FILE=EPFILE, STATUS='NEW', FORM='FORMATTED')
ENDIF
CLOSE(13)
OPEN(1,FILE=FESFILE, STATUS='OLD', FORM='FORMATTED')
OPEN(2,FILE=FMCFILE, STATUS='OLD', FORM='FORMATTED')
READ(1,10) ((FE(I,J), I=1,2), J=1,901)
READ(2,15) ((FM(I,J), I=1,11), J=1,1500)
10 FORMAT(1PE20.13,1X,E20.13)
15 FORMAT(11(1PE20.13,1X))
CLOSE(1)
CLOSE(2)
C      write input data to output file
OPEN(11,FILE=OUTFILE, STATUS='NEW', FORM='FORMATTED')
WRITE(11,20) DAY, HOUR, HEADER, N, NS, NEL, NMC, NT, NTURNS, NB, DEL, DELP,
1 INT, NPLOT, SIGD, SIGT, FESFILE, FMCFILE, INFILE, OUTFILE
20 FORMAT(' PROGRAM HMINUSINJ5 ',2A10,1X,A80/' N=',I8,' NS=',I8,
1 ' NEL=',I4,' NMC=',I4,' NT=',I2,' NTURNS=',I3,' NBINS=',I3,
2 ' DEL(mm)=',F5.3,' DELP(mr)=',F6.4,' INT=',I7,' NPLOT=',I5/
3 ' SIGD(mb)=',F7.3,' SIGT(mb)=',F7.3,' FESFILE=',A12,' FMCFILE=',
4 A12,' INFILE=',A12,' OUTFILE=',A12)
WRITE(11,30) P,TA,TAU,TZ,EX,EZ,W,H,XFO,NBC
30 FORMAT(' P(GeV/c)=',F8.6,' TA(amu)=',F9.6,' TAU(ug/cm2)=',F7.2,
1 ' TZ=',F3.0,' EX(mm-mm)=',F8.6,' EZ(mm-mm)=',F8.6/' W(mm)=',F5.2,
2 ' H(mm)=',F6.2,' XFO(mm)=',F5.2,' NBC=',I1)
WRITE(11,40) XNU0,ZNU0,AX,AZ,BX,BZ,TR,OMH,OMV,AH,AV,TI,TZ,ALFX,
1 ALFZ
40 FORMAT(' XNU=',F6.4,' ZNU=',F6.4,' AX(mm-mm)=',F6.2,' AZ(mm-mm)=',
1 F6.2,' BX(m)=',F6.3,' BZ(m)=',F6.3,' TR(mus)=',F6.4/' OMH(r/s)=',
2 F7.2,' OMV(r/s)=',F7.2,' AH(mm)=',F5.2,' AV(mm)=',F5.2,' TI(ms)=',
3 F7.5,' TF(ms)=',F7.5,' TIZ(ms)=',F7.5,' ALFX=',F7.4,' ALFZ=',F7.4)
WRITE(11,45) BUN,C,DNMX,DNMZ,SIGRX,SIGRZ,XNO
45 FORMAT(' BUN=',F4.3,' C(m)=',F8.3,' DNMX=',F4.3,' DNMZ=',F4.3,
1 ' SIGRX(mm)=',F6.2,' SIGRZ(mm)=',F6.2,' XNO=',1PE10.4)
C      preliminary. Ellipse sizes, matrix elements, phase space arrays.
GAMMAX=(1.0D0+ALFX**2)/BX
GAMMAZ=(1.0D0+ALFZ**2)/BZ
SIGBX=DSQRT(EX*BX)*1.0D-3
SIGBXP=DSQRT(EX*GAMMAX)*1.0D-3
SIGBZ=DSQRT(EZ*BZ)*1.0D-3
SIGBZP=DSQRT(EZ*GAMMAZ)*1.0D-3
SIGAX=DSQRT(AX*BX)*1.0D-3
SIGAXP=DSQRT(AX*GAMMAX)*1.0D-3
SIGAZ=DSQRT(AZ*BZ)*1.0D-3
SIGAZP=DSQRT(AZ*GAMMAZ)*1.0D-3
SIGRX=SIGRX*1.0D-3
SIGRZ=SIGRZ*1.0D-3
DO 50 J=1,NB
NX(J)=0
NTX(J)=0
NY(J)=0
50 NTY(J)=0
DO 55 J=1,NTURNS
TRAVERS(J)=0.0D0
55 LOSSTURN(J)=0
X(1)=-DFLOTJ(NB/2)*DEL*1.0D-3
Y(1)=X(1)
TX(1)=-DFLOTJ(NB/2)*DELP*1.0D-3

```

```
TY(1)=TX(1)
DO 60 J=2,NB
X(J)=X(J-1)+DEL*1.0D-3
Y(J)=X(J)
TX(J)=TX(J-1)+DELP*1.0D-3
60 TY(J)=TX(J)
CALL MCSCAT(0,NMC,NS,1.0D0,PM,P,TZ,TA,TAU,P,B,NT,TMS,TH)
CALL ELSCAT (0,NS,NEL,TH)
XXPZZP(1)=0.0D0
XXPZZP(3)=0.0D0
CALL TUNE (0,XXPZZP,XNU,ZNU,XM,ZM)
NLOST=0
NINT=0
NSCAT=0
NMIS=0
AH=AH*1.0D-3
AV=AV*1.0D-3
H=H*1.0D-3
TI=TI*1.0D-3
TIZ=TIZ*1.0D-3
TF=TF*1.0D-3
TR=TR*1.0D-6
W=W*1.0D-3
WHALF=W/2.0D0
HHALF=H/2.0D0
XF0=XF0*1.0D-3
I1=1
I2=INT
PROBINT=6.0221367D-10*TAU*SIGHT/TA
PROBSCAT=SIGD/SIGT
C      diagnostic print
      WRITE(11,61)
61 FORMAT(' SIGBX,SIGBXP,SIGBZ,SIGBZP,SIGAX,SIGAXP,SIGAZ,',
1' SIGAZP,XM11,XM12,XM21,XM22,ZM11,ZM12,ZM21,ZM22,NMC,NEL=')
      WRITE(11,62) SIGBX,SIGBXP,SIGBZ,SIGBZP,SIGAX,SIGAXP,SIGAZ,
1 SIGAZP,XM11,XM12,XM21,XM22,ZM11,ZM12,ZM21,ZM22,NMC,NEL
62 FORMAT(8(1PE15.6,1x)/8E14.6,2I6)
      WRITE(11,63) PROBINT,PROBSCAT,XNU,ZNU,SIGRX,SIGRZ,
1 (XM(J),J=1,4),(ZM(J),J=1,4)
63 FORMAT(' PROBINT=',1PE11.5,' PROBSCAT=',0PF7.5,' XNU=',
1 F8.5,' ZNU=',F8.5,' SIGRX(m)=',F7.5,' SIGRZ(m)=',F7.5/
2 ' XM(J),ZM(J)=',8(1PE11.4,1x))
C      main loop to select N points in time interval TF-TI
65 DO 200 I=I1,I2
C      select new particle coordinates relative to H-minus beam center
      XB=SIGBX*GASDEV(NS)
      XPB=SIGBXP*GASDEV(NS)
      ZB=SIGBZ*GASDEV(NS)
      ZPB=SIGBZP*GASDEV(NS)
      IF(DABS(XB).GT.WHALF.OR.DABS(ZB).GT.HHALF) THEN
          NMIS=NMISS+1
          GOTO 200
      ENDIF
C      modify new particle angles by foil scattering
      CALL MCSCAT(I,NMC,NS,1.0D0,PM,P,TZ,TA,TAU,P,B,NT,TMS,TH)
      PHI=TWOPI*RAND(NS)
      XPB=XPB+TH*DCOS(PHI)
      ZPB=ZPB+TH*DSIN(PHI)
      IF (RAND(NS).GT.PROBINT) GOTO 66
      NINT=NINT+1
```

```

IF (RAND(NS) .GT. PROBSCAT) GOTO 66
NSCAT=NSCAT+1
CALL ELSCAT (I, NS, NEL, TH)
PHI=TWOPI*RAND(NS)
XPB=XPB+TH*DCOS(PHI)
ZPB=ZPB+TH*DSIN(PHI)
C      transform new particle to admittance ellipse coordinates
66 T=TI+RAND(NS) * (TF-TI)
XC=AH*DEXP( - (T-TI)*OMH)
ZC=AV* (1.0D0-DEXP( - (T-TI+TIZ)*OMV) )
XXPZZP(1)=XFO+W/2.0D0-XC+XB
XXPZZP(2)=XPB-ALFX*XXPZZP(1)/BX
XXPZZP(3)=-ZC+ZB
XXPZZP(4)=ZPB-ALFZ*XXPZZP(3)/BZ
IF (NBC.EQ.0) THEN
    XXPZZP(2)=XPB
    XXPZZP(4)=ZPB
ENDIF
CALL TUNE (I,XXPZZP,XNU,ZNU,XM,ZM)
C determine time bin J in which new particle originated
DO 70 J=1,NTURNS
TUP=TI+DFLOTJ(J)*TR
IF (T.LE.TUP) GOTO 71
70 CONTINUE
71 TRAVERS(J)=TRAVERS(J)+1.0D0
C      transport particle around ring until XC+SIGAX < XFO
91 T=T+TR
IF (T.GT.TF) GOTO 97
TEMP=XXPZZP(1)
XXPZZP(1)=XM(1)*XXPZZP(1)+XM(2)*XXPZZP(2)
XXPZZP(2)=XM(3)*TEMP+XM(4)*XXPZZP(2)
TEMP=XXPZZP(3)
XXPZZP(3)=ZM(1)*XXPZZP(3)+ZM(2)*XXPZZP(4)
XXPZZP(4)=ZM(3)*TEMP+ZM(4)*XXPZZP(4)
XC=AH*DEXP( - (T-TI)*OMH)
ZC=AV* (1.0D0-DEXP( - (T-TI+TIZ)*OMV) )
XK=XXPZZP(1)+XC
ZK=XXPZZP(3)+ZC
IF (XK.LT.XFO.OR.XK.GT.XFO+W) GOTO 91
IF (ZK.LT.-H/2.0D0.OR.ZK.GT.H/2.0D0) GOTO 91
CALL MCSCAT(I,NMC,NS,1.0D0,PM,P,TZ,TA,TAU,P,B,NT,TMS,TH)
PHI=TWOPI*RAND(NS)
XXPZZP(2)=XXPZZP(2)+TH*DCOS(PHI)
XXPZZP(4)=XXPZZP(4)+TH*DSIN(PHI)
TRAVERS(J)=TRAVERS(J)+1.0D0
IF (RAND(NS) .GT. PROBINT) GOTO 91
NINT=NINT+1
IF (RAND(NS) .GT. PROBSCAT) GOTO 91
NSCAT=NSCAT+1
CALL ELSCAT (I, NS, NEL, TH)
PHI=TWOPI*RAND(NS)
XXPZZP(2)=XXPZZP(2)+TH*DCOS(PHI)
XXPZZP(4)=XXPZZP(4)+TH*DSIN(PHI)
GOTO 91
C      test if particle is outside admittance ellipses
97 IF(DABS(XXPZZP(1)).GT.SIGAX) GOTO 100
XPP=(-ALFX*XXPZZP(1)+DSQRT(SIGAX**2-XXPZZP(1)**2))/BX
XPM=(-ALFX*XXPZZP(1)-DSQRT(SIGAX**2-XXPZZP(1)**2))/BX
IF (XXPZZP(2).GT.XPP.OR.XXPZZP(2).LT.XPM) GOTO 100
IF (DABS(XXPZZP(3)).GT.SIGAZ) GOTO 100

```

```

ZPP=(-ALFZ*XXPZZP(3)+DSQRT(SIGAZ**2-XXPZZP(3)**2))/BZ
ZPM=(-ALFZ*XXPZZP(3)-DSQRT(SIGAZ**2-XXPZZP(3)**2))/BZ
IF(XXPZZP(4).GT.ZPP.OR.XXPZZP(4).LT.ZPM)GOTO 100
GOTO 110
100 NLOST=NLOST+1
      LOSSTURN(J)=LOSSTURN(J)+1
C      write NPLOT coordinates to EPFILE if NPLOT.Gt.0
110 IF(I.GT.NPLOT) GOTO 115
      WRITE(12,112) (XXPZZP(J), J=1,4)
112 FORMAT(4(F9.6,1x))
C      bin the particle in NX,NTX,NY,NTY arrays
115 DO 120 L=2,NB
      IF(XXPZZP(1).LE.X(L)) THEN
          NX(L-1)=NX(L-1)+1
          GOTO 130
      ENDIF
120 CONTINUE
      NX(NB)=NX(NB)+1
130 DO 140 L=2,NB
      IF(XXPZZP(2).LE.TX(L)) THEN
          NTX(L-1)=NTX(L-1)+1
          GOTO 150
      ENDIF
140 CONTINUE
      NTX(NB)=NTX(NB)+1
150 DO 160 L=2,NB
      IF(XXPZZP(3).LE.Y(L)) THEN
          NY(L-1)=NY(L-1)+1
          GOTO 170
      ENDIF
160 CONTINUE
      NY(NB)=NY(NB)+1
170 DO 180 L=2,NB
      IF(XXPZZP(4).LE.TY(L)) THEN
          NTY(L-1)=NTY(L-1)+1
          GOTO 200
      ENDIF
180 CONTINUE
      NTY(NB)=NTY(NB)+1
200 CONTINUE
C      CALL DATE(DAY)
      CALL TIME(HOUR)
      IF(I2.LT.N) GOTO 207
C      convert X,TX,Y,TY arrays back to mm and mrad
      DO 205 J=1,NB
          X(J)=X(J)*1.0D3
          TX(J)=TX(J)*1.0D3
          Y(J)=Y(J)*1.0D3
          TY(J)=TY(J)*1.0D3
C      write results to output file
207 WRITE(11,210) NLOST,TMS,B,NT,I2,NINT,NSCAT,DAY,HOUR,NMISS
210 FORMAT(1x,'NLOST=',I5,2x,'TMS(rad)=',F9.8,' B=',F7.4,' NT=',
1 I2,1x,' I2=',I8,' NINT=',I4,' NSCAT=',I4,' FINAL TIME=',2A10,
1 ' NMISS=',I6//,
2 3x,'X(mm)',6x,'NX',4x,'TX(mrad)'      'NTX',6x,'Y(mm)',6x,'NY',
3 4x,'TY(mrad)',5x,'NTY'//)
      WRITE(11,220) (X(J),NX(J),TX(J),NTX(J),Y(J),NY(J),TY(J),NTY(J),
1 J=1,NB)
220 FORMAT(2(F8.4,1x,I7,3x,F9.5,1x,I7,3x))
      IF(I2.LT.N) GOTO 260

```

```

DO 225 J=1,NTURNS
225 TRAVERS(J)=TRAVERS(J) / (DFLOTJ(N)/DFLOTJ(NTURNS))
      WRITE(11,230)
230 FORMAT(20x,'LOSSTURN DISTRIBUTION'//6(' TURN NLOST   TRAVERS ')//)
      L=NTURNS/6
      WRITE(11,240) (J,LOSSTURN(J),TRAVERS(J),L+J,LOSSTURN(L+J),
1 TRAVERS(L+J),2*L+J,LOSSTURN(2*L+J),TRAVERS(2*L+J),3*L+J,
2 LOSSTURN(3*L+J),TRAVERS(3*L+J),4*L+J,LOSSTURN(4*L+J),
3 TRAVERS(4*L+J),5*L+J,LOSSTURN(5*L+J),TRAVERS(5*L+J),J=1,L)
240 FORMAT(6(1x,I4,I6,2x,F7.3,1x))
      SUMTRAV=0.0D0
      DO 245 J=1,NTURNS
245 SUMTRAV=SUMTRAV+TRAVERS(J)
      AVTRAV=SUMTRAV/DFLOTJ(NTURNS)
      WRITE(11,250) DAY,HOUR,NS,AVTRAV
250 FORMAT(1x,'FINAL TIME=',2A10,3x,'FINAL SEED=',I8,' AVTRAV=',F8.3)
260 IF(I2.LT.N) THEN
      I1=I1+INT
      I2=I2+INT
      GOTO 65
    ENDIF
    CLOSE(11)
    IF(NPLOT.NE.0) CLOSE(12)
    CALL EXIT
  END

C ****
C      SUBROUTINE MCSCAT(IN,NMC,NS,PZ,PM,PP,TZ,TAU,P0,B,NT,TMS,TH)
C      Computes random multiple coulomb scattering angle THETA and proj-
C      ections TX and TY from a Moliere distribution. Formulation is given
C      in BNL Internal Report AGS DIV 71-1, Blumberg & Krausz (March, 1971)
C      This version uses subroutine FTABLE to generate the Moliere distri-
C      bution function F(D) for NMC points from a series of NT terms.
C      B = Moliere constant obtained by Newtons iteration.
C      IN = TEST NUMBER. IF IN=0 compute RMS multiple coulomb angle TMS
C      NMC= number of points desired in F(D) distribution function.
C      NS = seed integer for random number generator funtion RAND
C      NT = number of terms used by FTABLE to evaluate Moliere series
C      P0 = central momentum of incident beam (GeV/c)
C      PM = projectile rest mass (GeV/c**2)
C      PP = projectile momentum (GeV/c)
C      PZ = projectile atomic number z
C      TA = target atomic weight A (amu)
C      TAU= target areal density (ug/cm**2)
C      TH = random polar scattering angle THETA (rad)
C      TMS= RMS multiple coulomb scattering angle (rad)
C      TZ = target atomic number Z
C      IMPLICIT REAL*8 (A-H,O-Z)
C      DIMENSION D(1500),F(1500)
C          If IN=0 compute RMS multiple coulomb scattering angle TMS
C          IF (IN.EQ.0) GOTO 10
C          IF (PP.EQ.P0) GOTO 90
C          compute TMS
10 ZET=TZ+1.0D0
30 BETASQ=1.0D0/(1.0D0+(PM/PP)**2)
      T1SQRD=1.569149936D-13*TAU*ZET*TZ*PZ**2/(TA*BETASQ*PP**2)
      EPS=1.13D0+2.002251163D-4*(TZ*PZ)**2/BETASQ
      T1TASQ=8.838530658D-3*TAU*ZET*TZ**.333333*PZ**2/(TA*BETASQ*EPS)
C          compute Moliere's B using Newton's iteration
      CONST=DLOG(T1TASQ)-.154431329803066D0
      B0=1.0D+1

```

```
B=B0
40 IF (B.LE.0.0D0) THEN
    B0=B0/2.0D0
    IF (B0.LT.1.0D0) THEN
        B=1.0D0
        GOTO 60
    ELSE
        B=B0
    ENDIF
ENDIF
FOFB=B-DLOG(B)-CONST
IF (B.EQ.1.0D0) GOTO 60
BNEW=B*(B-FOFB-1.0D0)/(B-1.0D0)
IF (DABS(BNEW-B).LE.1.0D-6) GOTO 60
B=BNEW
GOTO 40
60 TMS=DSQRT(T1SQRD*B)
C      construct table of F=SUM(N=0,NT)Fn/B**n vs. D
CALL FTABLE (B,NMC,NT,D,F)
C      diagnostic print
C      WRITE(11,81)
C 81 FORMAT(3x,'I',8x,'D(I)',9x,'F(I)')
C      WRITE(11,82) (I,D(I),F(I), I=1,NMC)
C 82 FORMAT(I4,F12.4,F13.9)
DO 70 J=1,NMC
70 F(J)=F(J)/F(NMC)
C      select random angle THETA
90 R=RAND(NS)
DO 100 I=1,NMC
IF (R.LT.F(I)) GOTO 110
100 CONTINUE
TH=(D(NMC)+(D(NMC)-D(NMC-1))*(R-F(NMC))/(F(NMC)-F(NMC-1)))*TMS
GOTO 130
110 TH=(D(I-1)+(D(I)-D(I-1))*(R-F(I-1))/(F(I)-F(I-1)))*TMS
130 RETURN
END
C ****
SUBROUTINE FTABLE (B,NMC,NT,D,F)
C Evaluates Moliere distribution function F(D,B)=1-exp(-D**2)+
C SUM(n=1,NT)Fn(D)/B**n for subroutine MCSCAT. The tables Fn(D) are read
C by the main program as FM(J,K), J=1,11, K=1,1500 with FM(11,K)=D(K) and
C FM(1,K)=F1(K), FM(2,K)=F2(K), FM(3,K)=F3(K), ..., FM(10,K)=F10(K)
C in steps deltaD=.01 and transmitted to this subroutine in the form
C FM(J,K), K=1,1500, J=1,11 via COMMON/FMCTABLE. This program determines
C the maximum number of terms NT for which F is monotonically increasing
C with D and constructs F(K), K=1,NMC where NMC is number of points
C desired by MCSCAT for the F table. If NMC.LT.NDMAX=1500, data points in
C F are eliminated by determining whether the point can be evaluated by
C linear interpolation between neighboring points to specified accuracy
C EPS. If input NT=-N, compute series for NT=N. VAX REAL*8, 9/18/93.
IMPLICIT REAL*8 (A-H,O-Z)
DIMENSION D(1500),F(1500)
COMMON/FMCTABLE/FM(11,1500)
EPS=1.0D-10
C      determine number of terms NT in F series
DO 5 J=1,1500
5 D(J)=FM(11,J)
IF(NT.LE.0) THEN
    NT=-NT
    GOTO 90
```

```

ENDIF
IF(B.GE.3.0D0) THEN
    NT=10
    GOTO 90
ENDIF
IF(B.LE.1.0D0) THEN
    NT=0
    GOTO 90
ENDIF
NT=10
10 DO 30 J=1,1500
    F(J)=1.0D0-DEXP(-D(J)**2)
    DO 20 I=1,NT
20 F(J)=F(J)+FM(I,J)/B**I
30 CONTINUE
    DO 40 J=2,1500
    IF(F(J).GE.F(J-1)) GOTO 40
    IF(F(J-1)-F(J).LE.EPS) GOTO 40
    NT=NT-1
    GOTO 10
40 CONTINUE
C      reduce number of points in F table to NMC-70
50 NPOINTS=1500
NP=NPOINTS
60 DO 80 J=NPOINTS,3,-1
    IF(F(J)-F(J-1).GT.EPS) GOTO 80
    IF(NP.EQ.NMC-70) GOTO 85
    DO 70 K=J-1,NPOINTS
        D(K)=D(K+1)
70 F(K)=F(K+1)
NP=NP-1
80 CONTINUE
EPS=2.0D0*EPS
NPOINTS=NP
GOTO 60
C      add last 70 points as single scattering extrapolation
85 C=D(NMC-70)**2*(1.0D0-F(NMC-70))
J=NMC-69
DD=1.0D0
86 DO 87 K=1,10
    D(J)=D(J-1)+DD
    F(J)=1.0D0-C/D(J)**2
    IF(J.GE.NMC) GOTO 88
87 J=J+1
DD=2.0D0*DD
GOTO 86
C      if F(1) is not zero, set D(1)=F(1)=0 and increase NMC=NMC+1
88 IF(F(1).NE.0.0D0) THEN
    DO 89 J=NMC,1,-1
        D(J+1)=D(J)
89 F(J+1)=F(J)
        D(1)=0.0D0
        F(1)=0.0D0
        NMC=NMC+1
    ENDIF
    GOTO 120
C      evaluate F table when NT is known
90 DO 110 J=1,1500
    F(J)=1.0D0-DEXP(-D(J)**2)
    DO 100 I=1,NT

```

```
100 F(J)=F(J)+FM(I,J)/B**I
110 CONTINUE
    GOTO 50
120 RETURN
END
C ****
FUNCTION RAND(NSEED)
C Random numbers between 0.0 and 1.0. Set NSEED to any negative integer
C initially. From Numerical Recipes RAN2 routine, Press, Flannery, Teukol-
C sky & Vetterling, Cambridge Univ. Press (1987) 197.
IMPLICIT REAL*8 (A-H,O-Z)
INTEGER*4 M, IA, IC, IR(97), IFF, NSEED, IY, K
PARAMETER (M=714025, IA=1366, IC=150889, RM=1.0D0/M)
DATA IFF/0/
IF(NSEED.LT.0.OR.IFF.EQ.0) THEN
C           executed only on initial entry
    IFF=1
    NSEED=JMOD(IC-NSEED,M)
    DO 11 J=1,97
        NSEED=JMOD(IA*NSEED+IC,M)
        IR(J)=NSEED
11  CONTINUE
    NSEED=JMOD(IA*NSEED+IC,M)
    IY=NSEED
ENDIF
C           normal execution sequence on subsequent entries
K=1+(97*IY)/M
IF(K.GT.97.OR.K.LT.1) PAUSE
IY=IR(K)
RAND=IY*RM
NSEED=JMOD(IA*NSEED+IC,M)
IR(K)=NSEED
RETURN
END
C ****
FUNCTION GASDEV(NSEED)
C generates random numbers from a normalized Gaussian distribution
C p(y)=exp(-y**2/2)/sqrt(2*pi) with unit variance (sigma=1). From
C Numerical Recipes, Press, Flannery, Teukolsky & Vetterling, Camb.
C Univ. Press (1987) 203. Requires uniform random generator RAND.
C VAX REAL*8, 9/29/93.
IMPLICIT REAL*8 (A-H,O-Z)
INTEGER*4 NSEED
DATA ISET/0/
IF(ISET.EQ.0) THEN
1   V1=2.0D0*RAND(NSEED)-1.0D0
    V2=2.0D0*RAND(NSEED)-1.0D0
    R=V1**2+V2**2
    IF(R.GE.1.0D0) GOTO 1
    FAC=DSQRT(-2.0D0*DLOG(R)/R)
    GSET=V1*FAC
    GASDEV=V2*FAC
    ISET=1
ELSE
    GASDEV=GSET
    ISET=0
ENDIF
RETURN
END
C ****
```

SUBROUTINE ELSCAT (IN,NS,NEL,THLAB)
C Selects a random polar scattering angle THLAB from an elastic
C nuclear diffraction scattering distribution F derived from optical
C model of Fernbach, Serber & Taylor, Phys. Rev. 75 (1949) 1352. F is
C obtained from a pre-prepared table FE(J,K) in COMMON/FESTABLE/ and
C reduced to NEL values on first (IN=0) entry into routine. The tables
C FE(2,J) vs THL(rad)=FE(1,J) are specific to a given projectile,target
C nucleus, and projectile energy. NS is SEED for random generator.
C See also Blumberg & Krausz, BNL-24901(1971). VAX REAL*8, 10/23/93.

IMPLICIT REAL*8 (A-H,O-Z)
DIMENSION TH(901),F(901)
COMMON/FESTABLE/FE(2,901)
EPS=1.0D-10
IF(IN.NE.0) GOTO 50

C reduce length of TH and F tables to NEL normalized values
DO 10 J=1,901
TH(J)=FE(1,J)
10 F(J)=FE(2,J)/FE(2,901)
NPOINTS=901
NP=NPOINTS
20 DO 40 J=NPOINTS,3,-1
IF(F(J)-F(J-1).GT.EPS) GOTO 40
IF(NP.EQ.NEL) GOTO 50
DO 30 K=J-1,NPOINTS
TH(K)=TH(K+1)
30 F(K)=F(K+1)
NP=NP-1
40 CONTINUE
EPS=2.0D0*EPS
NPOINTS=NP
GOTO 20

C select random scattering angle THLAB
50 R=RAND(NS)
DO 60 J=2,NEL
IF (R.LT.F(J)) GOTO 70

60 CONTINUE
THLAB=TH(NEL)
GOTO 80

70 THLAB=TH(J-1)+(TH(J)-TH(J-1))*(R-F(J-1))/(F(J)-F(J-1))
80 RETURN
END

C ****
SUBROUTINE TUNE (IN,XXPZZP,XNU,ZNU,XM,ZM)
C computes horizontal and vertical tunes XNU and ZNU and one-turn
C transport matrices XM(1)=XM11,XM(2)=XM12,XM(3)=XM21,XM(4)=XM22,ZM(1)=
C ZM11,ZM(2)=ZM12,ZM(3)=ZM21,ZM(4)=ZM22 for a particle of rest energy
C PM(GeV/c**2) and momentum PP(GeV/c) at ellipse coordinate x(m)=
C XXPZZP(1) and z(m)=XXPZZP(3) and central tunes XNU0,ZNU0 for an
C assumed Gaussian charge distribution (unneutralized) in ring with
C circumference C(m) and XNO particles. B=bunching factor, ring betatron
C parameters ALFX,ALFZ,BX(m),BZ(m),EX(mm-mm),EZ(mm-mm). If IN=0 initial
C calculations are performed. Formulation follows H.Bruck, LA-TR-72-10,
C Chapt.XXVII and L.J.Laslett, BNL-7534(1963). If SIGRX and SIGRZ are
C zero, TUNE computes them from given DNM. If SIGRX and SIGRZ are non-
C zero, TUNE computes DNM (deltanuMAX) from them. VAX REAL*8, 11/8/93.

IMPLICIT REAL*8 (A-H,O-Z)
DIMENSION XXPZZP(4),XM(4),ZM(4)
COMMON/TUNEDAT/ALFX,ALFZ,B,BX,BZ,C,DNMX,DNMZ,EX,EZ,PM,PP,
1 SIGRX,SIGRZ,XNO,XNU0,ZNU0
PARAMETER(R0=1.534698558D-18,TWOPI=6.283185307179586D0,EPS=1.D-6)

IF (IN.NE.0) GOTO 20
C preliminary calculations if IN=0
BETASQ=1.0D0/(1.0D0+(PM/PP)**2)
GAMMA=1.0D0/DSQRT(1.0D0-BETASQ)
B2G3=BETASQ*GAMMA**3
CONST=R0*C*XN0/(TWOPI**2*B*B2G3)
RMX=DSQRT(EX*BX)*1.0D-3
RMZ=DSQRT(EZ*BZ)*1.0D-3
IF(SIGRX.NE.0.0D0.AND.SIGRZ.NE.0.0D0) GOTO 6
CX=DNMX*(XNU0-DNM)*RMX**2/CONST
CZ=DNMZ*(ZNU0-DNZ)*RMZ**2/CONST
ITER=0
UOLDX=1.0D0
1 C1=1.0D0-DEXP(-UOLDX)
UNEWX=(CX*C1**2-UOLDX**2*DEXP(-UOLDX))/(C1-UOLDX*DEXP(-UOLDX))
IF(DABS(UNEWX-UOLDX).LE.EPS) GOTO 2
UOLDX=UNEWX
ITER=ITER+1
IF(ITER.GT.20) GOTO 2
GOTO 1
2 IF(UNEWX.LT.0.0D0) THEN
SIGRX=0.5D0*RMX
GOTO 3
ENDIF
SIGRX=RMX/DSQRT(2.0D0*UNEWX)
3 ITER=0
UOLDZ=1.0D0
4 C1=1.0D0-DEXP(-UOLDZ)
UNEWZ=(CZ*C1**2-UOLDZ**2*DEXP(-UOLDZ))/(C1-UOLDZ*DEXP(-UOLDZ))
IF(DABS(UNEWZ-UOLDZ).LE.EPS) GOTO 5
UOLDZ=UNEWZ
ITER=ITER+1
IF(ITER.GT.20) GOTO 5
GOTO 4
5 IF(UNEWZ.LT.0.0D0) THEN
SIGRZ=0.5D0*RMZ
GOTO 8
ENDIF
SIGRZ=RMZ/DSQRT(2.0D0*UNEWZ)
GOTO 8
6 A0X=(0.5D0*CONST/SIGRX**2)/(1.0D0-DEXP(-0.5D0*RMX**2/SIGRX**2))
ARGX=XNU0**2-4.0D0*A0X
IF(ARGX.LT.0.0D0) THEN
DNMX=XNU0/2.0D0
GOTO 7
ENDIF
DNMX=(XNU0-DSQRT(ARGX))/2.0D0
7 A0Z=(0.5D0*CONST/SIGRZ**2)/(1.0D0-DEXP(-0.5D0*RMZ**2/SIGRZ**2))
ARGZ=ZNU0**2-4.0D0*A0Z
IF(ARGZ.LT.0.0D0) THEN
DNMZ=ZNU0/2.0D0
GOTO 8
ENDIF
DNMZ=(ZNU0-DSQRT(ARGZ))/2.0D0
8 TSXSQ=2.0D0*SIGRX**2
TSZSQ=2.0D0*SIGRZ**2
GAMMAX=(1.0D0+ALFX**2)/BX
GAMMAZ=(1.0D0+ALFZ**2)/BZ
CX=CONST/(1.0D0-DEXP(-RMX**2/TSXSQ))
CZ=CONST/(1.0D0-DEXP(-RMZ**2/TSZSQ))

C diagnostic print
C WRITE(11,10) CONST,RMX,RMZ,UNEWX,UNEWZ,UOLDX,UOLDZ,SIGRX,SIGRZ,
1 DNMX,DNMZ
10 FORMAT(' CONST=',1PE12.5,' RMX(m)=',E12.5,' RMZ(m)=',E12.5,' UN',
1' EWX=',E12.5,' UNEWZ=',E12.5,' UOLDX=',E12.5/' UOLDZ=',E12.5,' S',
2' IGRX(m)=',E12.5,' SIGRZ(m)=',E12.5,' DNMX=',E12.5,' DNMZ=',E12.5)
C compute tunes XNU,ZNU and matrices XM,ZM
20 IF (DABS(XXPZZP(1)).LE.EPS) THEN
 XNU=XNU0-DNMX
 GOTO 30
ENDIF
AX=CX*(1.0D0-DEXP(-XXPZZP(1)**2/TSXSQ))/XXPZZP(1)**2
ARGX=XNU0**2-4.0D0*AX
IF(ARGX.LT.0.0D0) THEN
 XNU=XNU0/2.0D0
 GOTO 30
ENDIF
XNU=(XNU0+DSQRT(ARGX))/2.0D0
30 IF (DABS(XXPZZP(3)).LE.EPS) THEN
 ZNU=ZNU0-DNMZ
 GOTO 40
ENDIF
AZ=CZ*(1.0D0-DEXP(-XXPZZP(3)**2/TSZSQ))/XXPZZP(3)**2
ARGZ=ZNU0**2-4.0D0*AZ
IF(ARGZ.LT.0.0D0) THEN
 ZNU=ZNU0/2.0D0
 GOTO 40
ENDIF
ZNU=(ZNU0+DSQRT(ARGZ))/2.0D0
40 ARGX=TWOPI*XNU
CARGX=DCOS(ARGX)
SARGX=DSIN(ARGX)
XM(1)=CARGX+ALFX*SARGX
XM(2)=BX*SARGX
XM(3)=-SARGX*GAMMAX
XM(4)=CARGX-ALFX*SARGX
ARGZ=TWOPI*ZNU
CARGZ=DCOS(ARGZ)
SARGZ=DSIN(ARGZ)
ZM(1)=CARGZ+ALFZ*SARGZ
ZM(2)=BZ*SARGZ
ZM(3)=-SARGZ*GAMMAZ
ZM(4)=CARGZ-ALFZ*SARGZ
RETURN
END

'TEST60 1GeV,N=1E7,1250TURNs,400ug/cm2,A=470mm-mm,EB=58.75mm-mm,8x4mm,NBC=1'
10000000,-206142,750,750,10,1250,300,2500000,20000,.5,.06
1.696037918,12.,400.,6.,.138,.138,8.,4.,46.,112.,370.,1
3.82,3.78,470.,470.,22.57,5.29,.79504,1108.67
1108.67,40.9,24.20781,0.,.9938,.181298,2.1237,-.5659
.324,208.558,.25,.25,0.,0.,1.042e14
'FES.d','FMC.d','hminus60.out'
'xxpzzp60.out'

Appendix B

PROGRAM TESTELKIN

```

C Test subroutine ELKIN. Relativistic Kinematics of elastic scattering
C N      = number of angles in TB table
C PA     = atomic weight (amu) of projectile M1
C SP     = total proton-proton cross section at T1 (millibarns)
C T1     = kinetic energy (MeV) of incident projectile M1
C TA     = atomic weight (amu) of target nucleus
C TH3    = lab angle of scattered projectile (rad)
C V      = depth of nuclear potential energy (MeV) of target nucleus
IMPLICIT REAL*8 (A-H,O-Z)
REAL*8 J3,K1R,K2R,K3R
CHARACTER*10 DAY,HOUR
CHARACTER*12 OUTFILe
CHARACTER*80 HEADER
DIMENSION TB(4,2000)
CALL DATE(DAY)
CALL TIME(HOUR)
WRITE(*,*) ' enter HEADER(A80)='
READ(*,*) HEADER
WRITE(*,*) ' enter PA,TA,T1,SP,V,TH3,N,OUTFILE(A12)='
READ(*,*) PA,TA,T1,SP,V,TH3,N,OUTFILE
OPEN(1,FILE=OUTFILE,STATUS='NEW',FORM='FORMATTED')
CALL ELKIN(PA,TA,T1,SP,V,TH3,N,K1R,K2R,K3R,TH3P,T3,J3,TB,SD)
WRITE(1,10)DAY,HOUR,HEADER,PA,TA,T1,SP,V,TH3,N,OUTFILE,K1R,K2R,
1 K3R,SD
10 FORMAT(1x,'PROGRAM TESTELKIN ',2A10,1x,A80/' PA(amu)=',F9.7,
1 ' TA(amu)=',F10.6,' T1(MeV)=',F9.3,' SP(mb)=',F5.2,' V(MeV)=',
2 F4.1,' TH3(rad)=',F6.4,' N=',I4,' OUTFILe=',A12/' K1R=',1PE11.5,
3 ' K2R=',E11.5,' K3R=',E11.5,' SD(mb)=',E13.5//2(' THETA(RAD) ',
4 ' THETAP(RAD)   T1(MeV)',10x,'J3',3x))
IF (TH3.NE.0.0D0) WRITE(1,20) TH3,TH3P,T3,J3
20 FORMAT(1x,F10.6,F12.6,F10.4,E12.4)
C L=N/2
C IF(N.GT.0)WRITE(1,30)(TB(1,J),TB(2,J),TB(3,J),TB(4,J),TB(1,L+J),
C 1 TB(2,L+J),TB(3,L+J),TB(4,L+J), J=1,L)
C 30 FORMAT(2(1x,F10.6,F12.6,F10.4,E12.4,3x))
IF(N.GT.0) WRITE(1,30) (TB(1,J),TB(2,J),TB(3,J),TB(4,J), J=1,N)
30 FORMAT(4(1PE20.13,1x))
CLOSE(1)
CALL EXIT
END
C *****
SUBROUTINE ELKIN(PA,TA,T1,SP,V,TH3,N,K1R,K2R,K3R,TH3P,T3,J3,TB,SD)
C Relativistic kinematics of elastic scattering M2(M1,M1)M2 of project-
C ile of mass PA(amu) on target TA(amu) at rest in lab frame. TA.GT.PA
C assumed. Returns table TB of CM scattered angle TH3P, lab energy T3
C (MeV) of scattered projectile M1(MeV), and CM to lab cross-section
C transformation J3. Also returns products of wavenumber X target nucl.
C radius R, K1R,K2R and K3R. K1 is the difference between wave number
C inside and outside nucleus, K1=k*(sqrt(1+V/T)-1) with V=depth of nucl.
C potential energy(MeV) and T=TCM=kinetic energy of reduced mass MU=M1*
C M2/(M1+M2) in CM=T1CM+T2CM. K2=k=PCM/hbar*c where PCM(MeV)=p*c and p
C is the CM momentum of the reduced mass. K3=3*TA*SIGPP/4*pi*R**3 with
C SIGPP=SP=proton-proton total cross-section(mb) at incident projectile
C lab kinetic energy T1(MeV). Target radius R=R0*(TA)**1/3 (fm). The
C kinematics are summarized in Blumberg & Krausz, BNL-24901(1971) and
C based on Blumberg & Schlesinger, LAMS-1718(1955). The total elastic
C cross-section SIGMADF=SD(mb) is given by optical model of Fernbach,
C Serber & Taylor(FST), Phys.Rev.75(1949)1352. Kinematics verified by
C PROGRAM KINLAMS.

```

```

C ALPHA=kinematic parameter (see LAMS-1718)
C J3=CM to lab solid angle transformation at TH3, dOMEgap/dOMEGA
C K1=k*(sqrt(1+V/T)+1) (see FST)
C K2=p/hbar, the wavenumber of reduced mass MU in CM frame
C K3=3(TA)sigmapp/4piR**3
C M1=rest energy(MeV) of incident projectile of mass PA(amu)
C M2=rest energy(MeV) of target nucleus of mass TA(amu)
C MU=reduced mass M1*M2/(M1+M2) in CM frame (MeV)
C M=M1+M2=total rest energy (MeV)
C N=number of increments of lab angle TH3(rad) in TB table
C PA=atomic weight of projectile M1 (in amu)
C PCM=CM momentum p*c (MeV) of reduced mass.
C R=radius of target nucleus (fm), R=R0*TA**1/3
C SD=total elastic diffraction cross-section(mb). (see FST)
C SP=total proton-proton cross-section(mb) at projectile lab energy T1
C TA=atomic weight of target nucleus (amu)
C TB=table of TH3P(rad),T3(MeV) and J3 vs.TH3(rad) if N.NE.0
C TCM=E-ECM=kinetic energy(MeV) of reduced mass MU in CM frame
C TH3=lab angle(rad) of scattered particle M1.
C TH3P=CM angle(rad) corresponding to lab angle TH3.
C T1=lab kinetic energy(MeV) of incident projectile M1.
C T3=lab kinetic energy(MeV) of scattered incident projectile at TH3
IMPLICIT REAL*8 (A-H,O-Z)
REAL*8 J3,K1R,K2R,K3R,M1,M2,M,MU
DIMENSION TB(4,2000)
AMUMEV=931.49432D0
R0=1.25D0
PI=3.141592653589793D0
M1=PA*AMUMEV
M2=TA*AMUMEV
M=M1+M2
MU=M1*M2/(M1+M2)
R=R0*TA**.33333333
A=DSQRT(M**2+2.0D0*M2*T1)
ALPHA=(M1**2+M1*M2+M2*T1)/(M2**2+M1*M2+M2*T1)
C compute wavenumber X R=K1R,K2R,K3R and total elastic cross-section SD
M21=M2/M1
G1=1.0D0+T1/M1
G2P=(M21+G1)/DSQRT(M21**2+2.0D0*M21*G1+1.0D0)
TCM=T1-M*(G2P-1.0D0)
PCM=DSQRT(TCM**2+2.0D0*MU*TCM)
PR2=1.0D1*PI*R**2
K3R=0.75D0*TA*SP/PR2
K2R=PCM*R/1.9732857D2
K1R=K2R*(DSQRT(1.0D0+V/TCM)-1.0D0)
C1=0.25D0*K3R**2+K1R**2
C2=2.0D0*K1R*C1+K1R*K3R
C3=0.25D0*K3R**2-K1R**2+C1*K3R
C4=1.0D0-(1.0D0+2.0D0*K3R)*DEXP(-2.0D0*K3R)
SD=PR2*(1.0D0+0.5D0*C4/K3R**2-(0.25D0*K3R**2-K1R**2+DEXP(-K3R)*
1 (C2*DSIN(2.0D0*K1R)-C3*DCOS(2.0D0*K1R)))/C1**2)
C diagnostic print
WRITE(1,5) A,ALPHA,PCM,TCM,PR2,C1,C2,C3,C4,R
5 FORMAT(' ELKIN DIAGNOSTIC PRINT'/' A=',1PE12.5,' ALPHA=',E12.5,
1 ' PCM=',E12.5,' TCM=',E12.5,' PR2=',E12.5/' C1=',E12.5,' C2=',E12.5,' C3=',E12.5,' C4=',E12.5,' R(fm)=',F8.5)
C compute table of TH3P,T3 and J3 vs. TH3 if N.NE.0
IF(N.EQ.0) GOTO 30
DTH3=PI/DFLOTJ(N)
TB(1,1)=0.0D0

```

```
DO 20 J=1,N
TANPSIS=((M+T1)*DTAN(TB(1,J))/A)**2
IF(TB(1,J).EQ.PI/2.0D0) THEN
  CTH3P=-ALPHA
  GOTO 10
ENDIF
S=1.0D0
IF(TB(1,J).GT.PI/2.0D0) S=-S
CTH3P=(-ALPHA*TANPSIS+S*DSQRT(1.0D0-(ALPHA**2-1.0D0)*TANPSIS))/  
1 (1.0D0+TANPSIS)
10 TB(2,J)=DACOS(CTH3P)
TB(3,J)=((M1*M+M2*T1)*(M+T1)+M2*T1*(T1+2.0D0*M1)*CTH3P)/A**2-M1
ST1=DSQRT(T1**2+2.0D0*M1*T1)
ST3=DSQRT(TB(3,J)**2+2.0D0*M1*TB(3,J))
TB(4,J)=M2*ST1*((M+T1)*ST3-(M1+TB(3,J))*ST1*DCOS(TB(1,J)))/  
1 (A*ST3)**2
20 TB(1,J+1)=TB(1,J)+DTH3
C compute CM angle TH3P, lab energy T3 and transformation J3 if TH3>0
30 IF(TH3.LE.0.0D0) GOTO 50
  TANPSIS=((M+T1)*DTAN(TH3)/A)**2
  IF(TH3.EQ.PI/2.0D0) THEN
    CTH3P=-ALPHA
    GOTO 40
  ENDIF
  S=1.0D0
  IF(TH3.GT.PI/2.0D0) S=-S
  CTH3P=(-ALPHA*TANPSIS+S*DSQRT(1.0D0-(ALPHA**2-1.0D0)*TANPSIS))/  
1 (1.0D0+TANPSIS)
40 TH3P=DACOS(CTH3P)
T3=((M1*M+M2*T1)*(M+T1)+M2*T1*(T1+2.0D0*M1)*CTH3P)/A**2-M1
ST1=DSQRT(T1**2+2.0D0*M1*T1)
ST3=DSQRT(T3**2+2.0D0*M1*T3)
J3=M2*ST1*((M+T1)*ST3-(M1+T3)*ST1*DCOS(TH3))/(A*ST3)**2
50 RETURN
END
```

- 65 -
Appendix C

RELATIVISTIC KINEMATICS OF M2(M1,M3)M4 REACTION, PROGRAM TSTELKIN
 elastic scattering, protons + C12, T1=1000-MeV
 M1=938.272310 M2=11177.931840 M3=938.272310 M4=11177.931840 (MEV/C**2)

| THETA3 (rad) | ENERGY T3 (MEV) | THETA3P (CM ANGLE, radians) | J3 (LAB TO CM TRANSFORMATION) |
|------------------|--------------------|--------------------------------|----------------------------------|
| 0.0000 | 1000.000000 | 0.000000 | 7.386347E-01 |
| 0.0100 | 999.987133 | 0.011635 | 7.386472E-01 |
| 0.0200 | 999.948535 | 0.023271 | 7.386849E-01 |
| 0.0300 | 999.884214 | 0.034906 | 7.387476E-01 |
| 0.0400 | 999.794182 | 0.046540 | 7.388354E-01 |
| 0.0500 | 999.678459 | 0.058173 | 7.389483E-01 |
| 0.0600 | 999.537066 | 0.069806 | 7.390863E-01 |
| 0.0700 | 999.370033 | 0.081437 | 7.392494E-01 |
| 0.0800 | 999.177394 | 0.093068 | 7.394376E-01 |
| 0.0900 | 998.959186 | 0.104696 | 7.396508E-01 |
| 0.1000 | 998.715455 | 0.116323 | 7.398891E-01 |
| 0.1100 | 998.446249 | 0.127948 | 7.401525E-01 |
| 0.1200 | 998.151623 | 0.139570 | 7.404409E-01 |
| 0.1300 | 997.831635 | 0.151191 | 7.407543E-01 |
| 0.1400 | 997.486350 | 0.162809 | 7.410928E-01 |
| 0.1500 | 997.115836 | 0.174424 | 7.414563E-01 |
| 0.1600 | 996.720170 | 0.186036 | 7.418448E-01 |
| 0.1700 | 996.299429 | 0.197645 | 7.422583E-01 |
| 0.1800 | 995.853697 | 0.209251 | 7.426968E-01 |
| 0.1900 | 995.383064 | 0.220854 | 7.431603E-01 |
| 0.2000 | 994.887624 | 0.232453 | 7.436487E-01 |
| 0.2100 | 994.367475 | 0.244048 | 7.441620E-01 |
| 0.2200 | 993.822721 | 0.255639 | 7.447003E-01 |
| 0.2300 | 993.253470 | 0.267226 | 7.452635E-01 |
| 0.2400 | 992.659835 | 0.278808 | 7.458515E-01 |
| 0.2500 | 992.041934 | 0.290386 | 7.464645E-01 |
| 0.2600 | 991.399888 | 0.301959 | 7.471023E-01 |
| 0.2700 | 990.733824 | 0.313528 | 7.477649E-01 |
| 0.2800 | 990.043873 | 0.325091 | 7.484523E-01 |
| 0.2900 | 989.330172 | 0.336649 | 7.491645E-01 |
| 0.3000 | 988.592860 | 0.348201 | 7.499015E-01 |
| 0.3100 | 987.832081 | 0.359748 | 7.506632E-01 |
| 0.3200 | 987.047985 | 0.371288 | 7.514496E-01 |
| 0.3300 | 986.240723 | 0.382823 | 7.522607E-01 |
| 0.3400 | 985.410453 | 0.394352 | 7.530965E-01 |
| 0.3500 | 984.557337 | 0.405874 | 7.539568E-01 |
| 0.3600 | 983.681539 | 0.417390 | 7.548418E-01 |
| 0.3700 | 982.783228 | 0.428899 | 7.557514E-01 |
| 0.3800 | 981.862577 | 0.440401 | 7.566855E-01 |
| 0.3900 | 980.919764 | 0.451896 | 7.576441E-01 |
| 0.4000 | 979.954969 | 0.463384 | 7.586271E-01 |
| 0.4100 | 978.968377 | 0.474865 | 7.596346E-01 |
| 0.4200 | 977.960175 | 0.486338 | 7.606665E-01 |
| 0.4300 | 976.930554 | 0.497803 | 7.617228E-01 |
| 0.4400 | 975.879711 | 0.509260 | 7.628034E-01 |
| 0.4500 | 974.807843 | 0.520710 | 7.639083E-01 |
| 0.4600 | 973.715152 | 0.532151 | 7.650374E-01 |
| 0.4700 | 972.601844 | 0.543583 | 7.661907E-01 |
| 0.4800 | 971.468126 | 0.555008 | 7.673682E-01 |
| 0.4900 | 970.314211 | 0.566423 | 7.685698E-01 |
| 0.5000 | 969.140312 | 0.577830 | 7.697955E-01 |
| 0.5100 | 967.946646 | 0.589227 | 7.710452E-01 |

| | | | |
|--------|------------|----------|--------------|
| 0.5200 | 966.733436 | 0.600616 | 7.723189E-01 |
| 0.5300 | 965.500902 | 0.611995 | 7.736165E-01 |
| 0.5400 | 964.249272 | 0.623365 | 7.749380E-01 |
| 0.5500 | 962.978774 | 0.634725 | 7.762833E-01 |
| 0.5600 | 961.689638 | 0.646075 | 7.776524E-01 |
| 0.5700 | 960.382099 | 0.657416 | 7.790452E-01 |
| 0.5800 | 959.056392 | 0.668746 | 7.804616E-01 |
| 0.5900 | 957.712756 | 0.680067 | 7.819017E-01 |
| 0.6000 | 956.351432 | 0.691377 | 7.833653E-01 |
| 0.6100 | 954.972661 | 0.702676 | 7.848523E-01 |
| 0.6200 | 953.576689 | 0.713965 | 7.863628E-01 |
| 0.6300 | 952.163763 | 0.725243 | 7.878967E-01 |
| 0.6400 | 950.734131 | 0.736511 | 7.894538E-01 |
| 0.6500 | 949.288044 | 0.747767 | 7.910342E-01 |
| 0.6600 | 947.825754 | 0.759012 | 7.926377E-01 |
| 0.6700 | 946.347516 | 0.770246 | 7.942643E-01 |
| 0.6800 | 944.853585 | 0.781469 | 7.959140E-01 |
| 0.6900 | 943.344217 | 0.792680 | 7.975865E-01 |
| 0.7000 | 941.819673 | 0.803879 | 7.992820E-01 |
| 0.7100 | 940.280211 | 0.815067 | 8.010002E-01 |
| 0.7200 | 938.726093 | 0.826243 | 8.027411E-01 |
| 0.7300 | 937.157581 | 0.837406 | 8.045047E-01 |
| 0.7400 | 935.574939 | 0.848558 | 8.062908E-01 |
| 0.7500 | 933.978432 | 0.859698 | 8.080993E-01 |
| 0.7600 | 932.368324 | 0.870825 | 8.099303E-01 |
| 0.7700 | 930.744883 | 0.881939 | 8.117835E-01 |
| 0.7800 | 929.108375 | 0.893041 | 8.136590E-01 |
| 0.7900 | 927.459069 | 0.904131 | 8.155565E-01 |
| 0.8000 | 925.797232 | 0.915207 | 8.174761E-01 |
| 0.8100 | 924.123135 | 0.926271 | 8.194175E-01 |
| 0.8200 | 922.437047 | 0.937322 | 8.213809E-01 |
| 0.8300 | 920.739237 | 0.948360 | 8.233659E-01 |
| 0.8400 | 919.029977 | 0.959384 | 8.253725E-01 |
| 0.8500 | 917.309538 | 0.970396 | 8.274007E-01 |
| 0.8600 | 915.578189 | 0.981394 | 8.294503E-01 |
| 0.8700 | 913.836203 | 0.992378 | 8.315212E-01 |
| 0.8800 | 912.083850 | 1.003349 | 8.336132E-01 |
| 0.8900 | 910.321401 | 1.014306 | 8.357264E-01 |
| 0.9000 | 908.549128 | 1.025250 | 8.378605E-01 |
| 0.9100 | 906.767301 | 1.036179 | 8.400155E-01 |
| 0.9200 | 904.976191 | 1.047095 | 8.421912E-01 |
| 0.9300 | 903.176070 | 1.057997 | 8.443876E-01 |
| 0.9400 | 901.367205 | 1.068885 | 8.466044E-01 |
| 0.9500 | 899.549869 | 1.079759 | 8.488416E-01 |
| 0.9600 | 897.724329 | 1.090618 | 8.510990E-01 |
| 0.9700 | 895.890854 | 1.101463 | 8.533765E-01 |
| 0.9800 | 894.049713 | 1.112294 | 8.556740E-01 |
| 0.9900 | 892.201174 | 1.123111 | 8.579914E-01 |
| 1.0000 | 890.345502 | 1.133913 | 8.603284E-01 |
| 1.0100 | 888.482964 | 1.144700 | 8.626850E-01 |
| 1.0200 | 886.613825 | 1.155473 | 8.650610E-01 |
| 1.0300 | 884.738350 | 1.166231 | 8.674563E-01 |
| 1.0400 | 882.856802 | 1.176974 | 8.698708E-01 |
| 1.0500 | 880.969443 | 1.187703 | 8.723042E-01 |
| 1.0600 | 879.076535 | 1.198417 | 8.747564E-01 |
| 1.0700 | 877.178339 | 1.209116 | 8.772273E-01 |
| 1.0800 | 875.275112 | 1.219800 | 8.797168E-01 |
| 1.0900 | 873.367114 | 1.230469 | 8.822245E-01 |
| 1.1000 | 871.454602 | 1.241122 | 8.847505E-01 |
| 1.1100 | 869.537830 | 1.251761 | 8.872945E-01 |

- 67 -

Appendix D

```
PROGRAM SLOPE2
  compute slope of ellipse at stripper foil from dipoles B1 and B2.
  IMPLICIT REAL*8 (A-H,O-Z)
  REAL*8 L
  WRITE(*,*) 'enter GD,GF,R,L,D,D1,D2,D3,XF'
  READ(*,*) GD,GF,R,L,D,D1,D2,D3,XF
10  WRITE(*,*) 'enter T1,T2,DT1,DT2'
  READ(*,*) T1,T2,DT1,DT2
  IF(T1.EQ.0.0D0) GOTO 30
  SD=GD*L/R
  SF=GF*L/R
  TD=D1*SD*T1
  IF(T2.EQ.0.0D0) THEN
    T2=(XF-T1*(D+D1+D*D1*SD))/(D-D2)
  ELSE
    XF=T1*(D+D1+D*D1*SD) + T2*(D-D2)
  ENDIF
  TF=XF*SF
  TS=T1+T2+TD-TF
  XS=XF+D3*TS
  IF(DT1.EQ.0.0D0) THEN
    S=0.0D0
    GOTO 15
  ELSE
    DXF=DT1*(D+D1+D*D1*SD) + DT2*(D-D2)
    DTF=SF*DXF
    DTS=DT1*(1.0D0+D1*SD) + DT2 - DTF
    DXS=DXF + D3*DTS
    S=DTS/DXS
  ENDIF
15  WRITE(*,20) T1,T2,TF,TS,TD,XF,XS,S
20  FORMAT(' T1=',F7.5/' T2=',F7.5/' TF=',F7.5/' TS=',F8.5/
1   ' TD=',F8.5/' XF=',F7.5/' XS=',F7.5/' S=',F9.6//)
25  WRITE(*,*) 'enter T3,T4,D4,D5,D6'
  READ(*,*) T3,T4,D4,D5,D6
  IF(T3.EQ.0.0D0) GOTO 10
  XB3=XS+D4*TS
  T3F=TS+T3
  XB4=XB3+D5*T3F
  T4F=T3F+T4
  XB5=XB4+D6*T4F
  WRITE(*,26) XB3,XB4,XB5,T3F,T4F
26  FORMAT(' XB3=',F7.5/' XB4=',F7.5/' XB5=',F7.5/' T3F=',F7.5/
1   ' T4F=',F7.5//)
  GOTO 25
30  STOP
END
```